THE EFFECT OF NOTCH GEOMETRY ON FRACTURE BEHAVIOR OF GLASS FIBER REINFORCED POLYSTER

by

Faruk ELALDI

B.S. in M.E., Boğaziçi Üniversitesi,1983

Submitted to the Institute for Graduate Studies in Science and Engineering in Partial Fulfillment of the requirements for the degree of

Master of Science

in

Mechanical Engineering

Boğaziçi University

1986

ACKNOWLEDGEMENTS

I would like to express my feelings of sincere gratitute to my thesis supervisor, Associate Prefessor Öktem VARDAR for his invaluable guidance and friendly cooperation in the absence of which, the present work would not be possible at all.

Faruk ELALDI

June, 1986

ABSTRACT

The aim of this study is to determine quantitatively fracture toughness properties as a function of the crack tip radius, and the effect of fatigue damage produced at the crack tip to the critical stress intensity factor, and to examine the fracture behavior of randomly oriented-short-glass-fiber composite.

Apart from the intersection of the 5 percent secant line with the load vs displacement curve, two other critical points are observed. These are characterized as the debonding point, and the unstable crack propagation point. Thus, besides evaluating the K_Q value using the ASTM standard, two other stress intensity factors are utilized based on the above mentioned critical points.

The effect of notch root radius on fracture properties is observed to be insignificant in the notch root radius range 0.25-2.5 mm for GRP, but not negligible for the polymer matrix. Prior cyclic loading strongly influences the toughness behavior since debonding damage is incurred at the notch root.

ÖZET

Bu çalışmanın amacı cam elyafı ile gelişigüzel yönlerde takviye edilmiş plastiklerin kırılma tokluğu ile ilgili özelliklerinin, çatlak ucunun yuvarlaklığı ve yine bu uçta yaratılmış yorulma hasar bölgesiyle nasıl değiştiğini saptamak, böylece bu tür malzemelerin kırılma davranışları hakkında bilgi sahibi olmaktır.

Yüzde beş sekant çizgisinin, P_{VS} eğrisini kesmesinden ayrı olarak, diğer iki kritik nokta gözlenmektedir. Bunlar elyaf /polyester ara yüzeylerinin kopmaya başladığı nokta ve sabit olmayan çatlak ilerlemesinin başladığı noktadır. Böylece, kırılma tokluğu değerinin ASTM standardına göre hesaplanmasının yanında, bu diğer iki kritik noktayı referans alan iki ayrı gerilme şiddet faktörü hesaplanmaktadır.

Bu yaklaşımların sonucu olarak, çatlak ucu yuvarlaklığının, 0.25-2.5 mm.lik çentik ucu yuvarlaklığı aralığında, kırılma özellikleri üzerine önemli sayılmayacak bir etkisi olduğu tesbit edilmektedir. Bu etki polimer matriksler için ihmal edilmeyecek kadar büyüktür. Elyaf/polyster ara yüzeylerinin ayrılmasıyla ortaya çıkan hasar nedeniyle, yorulma yüklemesi malzemenin tokluk davranışını önemli derecede etkilemektedir.

TABLE OF CONTENTS

Page

LIST OF FIGURES

LIST OF TABLES

LIST OF SYMBOLS

a_o	Initial crack length for SE(T) specimen
af	Crack length corresponding to the which is considered
a/w	Crack length-the width of specimen ratio
B	Thickness of the specimens
C	Compliance
Lg	Gage length
L_t	Tab length
g	Notch tip radius
r_y	Radius of yield zone
r_D	Radius of debonding zone
σ	Tensile nominal stress
K	Stress intensity factor
K_Q	Candidate critical stress intensity factor
KIC	Fracture toughness ($kg/mm^{-3/2}$)
K_D	Debonding stress intensity factor
CSM	Chopped strand materials
N	Number of cycles
δ	Crack mouth displacement
V_f	Fibre volume percent

I. INTRODUCTION

Recent developments in processing and manufacturing technology of short fiber reinforced composites have led to a wide range of engineering applications of this class of materials to advanced structures and components.

From reliability and durability points of view, the fracture resistance of random short-fibre reinforced composites (SMC; sheet Molding Compound, CSM; Chopped Strand Materials, for example) is utmost importance in design and analysis of the composite materials and structures. Because of the relatively new entry of this material, studies of the fracture behavior of short-fiber composites have not been extensive. The mechanics and mechanisms of failure in this class of materials have not been fully understood.

Despite the microscopic heterogeneity among fibers, resin matrix, and calcium-carbonate filler, the chopped strand reinforcing glass fibers being statistically randomly oriented in the composite, macroscopic planar isotropy of thermal and mechanical properties is generally assumed.

The study of the Fracture Mechanics of composites has tended to branch into two areas, Micro-Fracture Mechanics and Macro-Fracture Mechanics. In the first area [3] several workers have associated fracture with such mechanisms as debonding, fiber pull-out and fiber fracture. In the second area, some other workers [1,2] have used the linear elastic fracture mechanics approach to investigate the effect of a crack on the failure of reinforced plastics.

Wu [1] and Beamont [2] have looked at the effect of varying crack length. Wu considered the case of a unidirectional glass reinforced epoxy resin matrix with a crack positioned parallel to the fibers and found that the critical stress intensity factor (K_c) did not vary significantly with crack length. Beamont and Phillips [2] in their test on carbon fiber reinforced epoxy resin and glass chopped strand mat reinforced polyster resin reached no firm conclusions regarding the effect of crack length on K_c values.

If it could be shown that the stress intensity approach can be applied to composites, then it may be possible to further exploit the considerable volume of theoretical and experimental work which has been carried out on isotropic materials. Little is known about the effects of crack-tip radius and the damage produced by fatigue on the fracture behavior of these kinds of materials. In metals, on the other hand the static tensile strengths of the materials are known to be reduced in the presence of notches or flows. The extent of decrease in strength is shown to be influenced by the sharpness of the notch. [4-12]

II. GENERAL CHARACTERISTICS OF DISCONTINUOUS-FIBER COMPOSITES

2.1 TYPES OF DISCONTINUOUS-FIBER COMPOSITES

The combination of short discontinuous fiber (from say, 3 to 30 mm in length) with thermoplastics or thermosettings as matrixes are of increasing technological interest, because the resultant materials can be processed by injection molding, compression molding or extrusion techniques generally similar to those used for polymers themselves.

The most common fibrous reinforcements are glass,graphitized carbon, and acicular minerals such as asbestos; sometimes glass/carbon hybrids are used as well. A wide range of fiber concentrations and geometrical arrays are used, depending on the application. [13].

One common type is a composite containing from 2 to 40 percent (by weight) of fibrous materials that can be injection molded; considerable orientation in the flow direction may be expected with this type. Fibers are usually 2-10 mm long for this type of composites.

A second common type is based on the impregnation of a

more or less isotropic mat that is made by laying-up short fibers (typically, chopped strands of 20-30 mm in length) in a random manner, impregnating the mat with a prepolymer, and curing the matrix. The mechanical response in such a case will be essentially isotropic, but the properties in a given direction will be lower than in the case of preferential fiber orientiation along the stress axis. Of course, chopped strands can be laid up to yield anisotropic specimens as well and short fibers are often blended with long fibers and particulate fillers. In fact, the combination of low cost with good strength, stiffness, fatigue resistance, and dimensional stability of short fiber reinforced plastics, especially relative to their density, has led to a major penetration in markets previously held by metals.

2.2 FRACTURE BEHAVIOR OF THE MATERIAL

Fracture of almost all randomly oriented short-glass-fiber reinforced composites have been observed to occur after the damage resulting from the fiber-matrix debonding. The debonding at the crack-tip initiates at loads much lower than the maximum fracture loads.

Initially, the crack-tip zone is quite transparent and when the load is gradually increased, a translucent zone initiates at the crack tip. The size of this translucent zone increases as the load is increased, and finally spreads along the plane of the crack to such an extent that unstable fracture occurs. This translucent zone is an indication of debonding

in the vicinity of the crack-tip.

The initiation of debonding in the crack-tip area can not be observed as a discontinuity point on the load-displacement curve of the material. The curve extends continuously to the point of unstable crack propagation. (Figure 2.1)

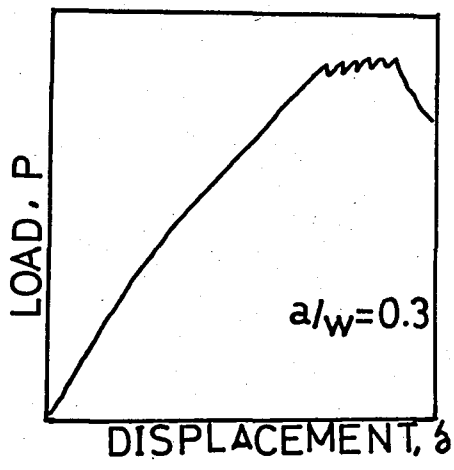

FIGURE 2.1 Schematic of Load-Displacement Curve for Fracture Tests of Randomly oriented glass-fiber reinforced Composite

A small region of nonlinearity is observed on the curve prior to the final fracture due to the presence of notch-tip damage. In general, very little stable crack growth is observed in static fracture tests of the notched composites under mode-I loading.

The initiation of debonding (damage) at the crack tip can be studied by loading a notched specimen (a/w = 0.3) to various fractions of its ultimate fracture load and then by examining the region near the crack-tip with a travelling microscope. By this procedure, it is found that the damage initiates at 60-65 percent of the fracture load [3]. Pictures of damage near the crack tip can be seen in figure 2.2

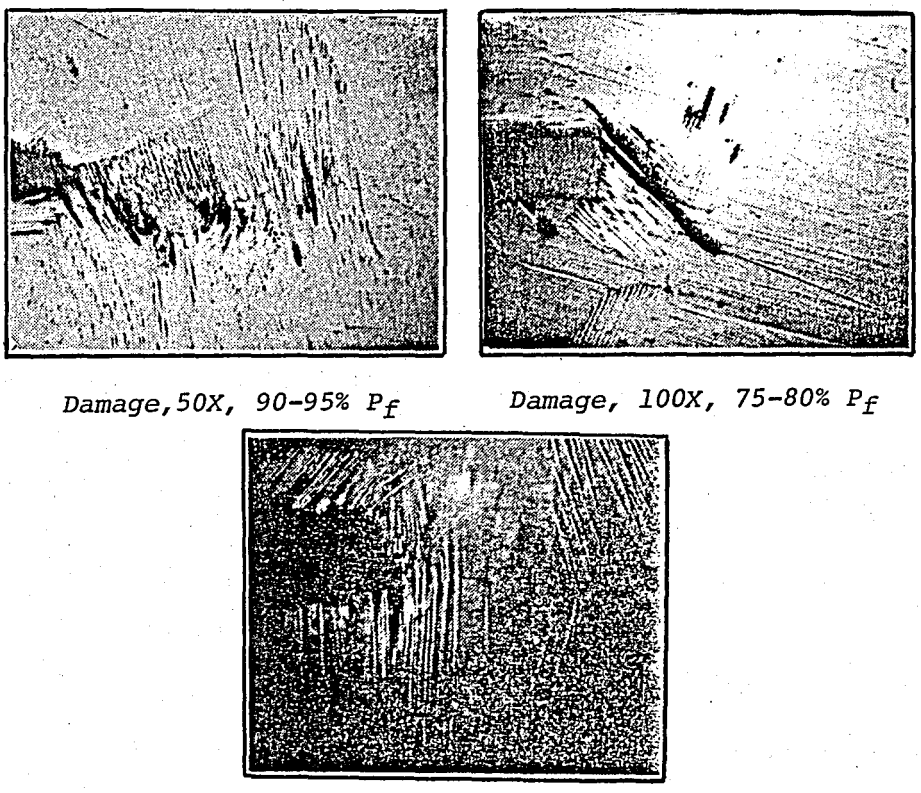

Damage,50X, 90-95% P_f

Damage, 100X, 75-80% P_f

Damage, 100X, 65-70% P_f

FGURE 2.2 Damage Near Crack Tip [4]

After final fracture, the pulled out fibers are seen at fracture surfaces as shown in figure 2.3

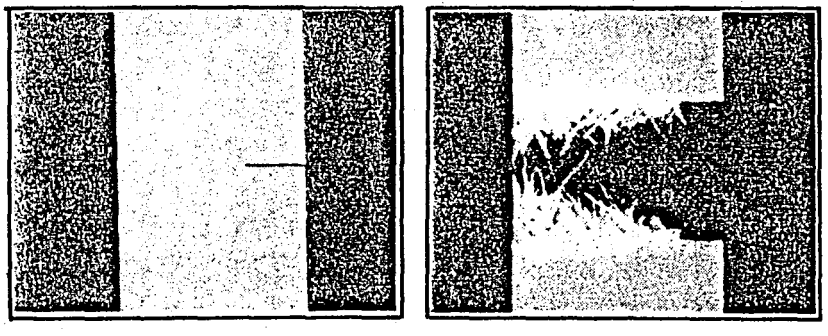

(a) *(b)*

FIGURE 2.3 A Typical Fracture Picture of Random Short-Fiber Reinforced Composite; (a) Virgin specimen (b) Mode-I Fracture (a_o=15 mm)

2.3 FACTORS AFFECTING FRACTURE TOUGHNESS

The tables and graphs presented in this section refer to the randomly oriented short-glass fiber reinforced brittle resins.

2.3.1 The Effect of Loading Conditions

Two types of gripping commonly used in testing are the wedge type and the pin loaded type. These gripping configurations are shown in Figure 2.4. For both pin-loaded and wedge type gripping arrangements, two 1 in. square pieces (tabs) are bonded to the specimen ends to avoid bearing failure at the loading points.

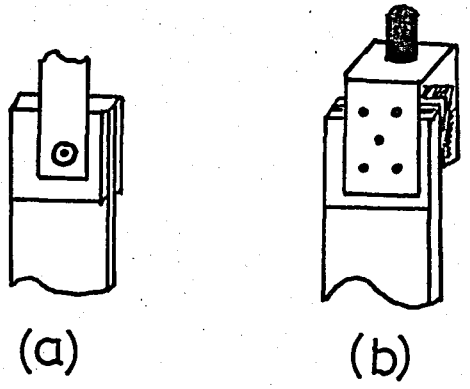

FIGURE 2.4 The Gripping Configurations :
(a) Pin-loaded type
(b) wedge type

Table 2.1 lists the effect of loading conditions on the candidate critical stress intensity factor, K_Q. [3] It is seen from these results that the K_Q values are the same for both end conditions.

TABLE 2.1 Effect of Loading Conditions on K_Q of the composite [3]

Wedge Grip Loaded			Pin loaded
Gage length, K_Q			Gage length, K_Q
7in	5in	3in	3in
9.3	9.3	9.3	9.9
	($ksi.in^{1/2}$)		
9.6	10.2	9.6	($ksi.in^{1/2}$) 9.8
9.2	9.3	9.8	9.7
9.2	9.2	10.4	9.9

(V_f = 0.29, a/w = 0.4)

2.3.2 The Effect of Crack Size

Figure 2.5 shows the K_Q values plotted against the crack size for the brittle resin/glass fiber composites. The candidate critical stress intensity factor decreases as a/w decreases. At larger crack lengths (a/w>0.2) the K_Q values are almost independent of the starter crack length. [3]

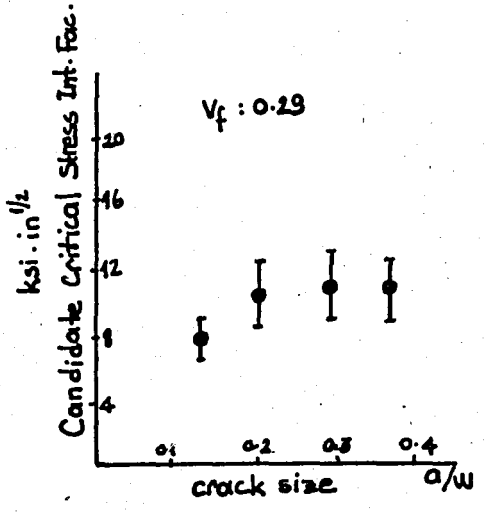

FIGURE 2.5 Variation of K_Q with Crack Size for SE(T) specimen [3]

2.3.3 The Effect of Fiber Concentration

Figure 2.6 shows the variation of the candidate critical stress intensity factor values with fiber volume concentration for randomly oriented short-glass-fiber reinforced brittle resin composites. The K_Q values increase with increasing fiber concentration. [4]

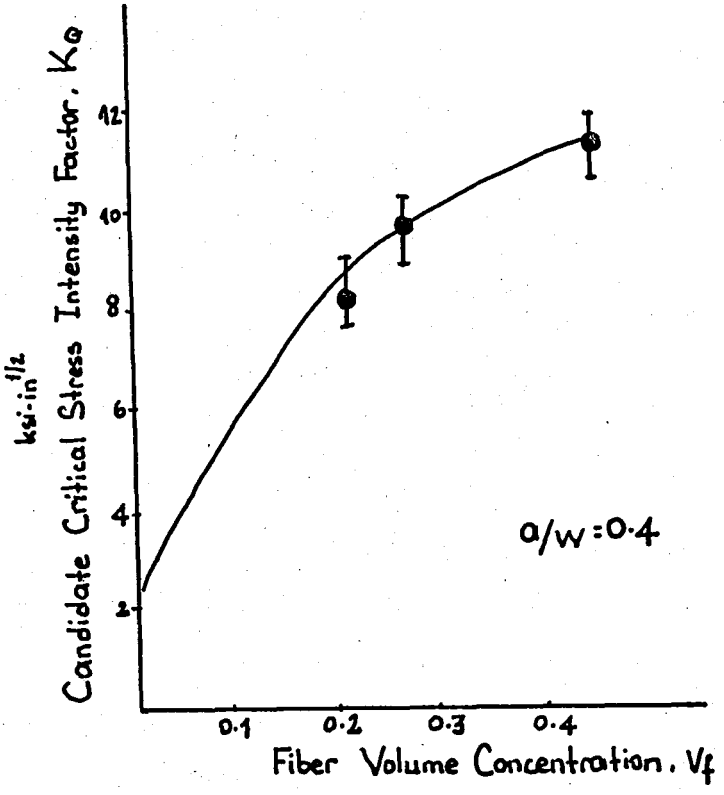

FIGURE 2.6 Variation of K_Q with fiber volume fraction for glass/epoxy Composites. [4]

2.3.4 The Effect of Thickness

The fracture toughness of metallic materials is known to depend on the thickness of the test specimen. Plane-stress conditions exist at the crack tip for very thin specimens, whereas for thicker specimens, plane-strain conditions can exist in the center of the sheet at the crack tip. [4]

In composites, the situation is different. Figure 2.7 shows the candidate critical stress intensity factor as a function of specimen thickness for a short-glass fiber/ brittle resin composite. The values of K_Q are independent of the thickness in the range of 1.27-5.0 mm. The crack propagation is in the plane of the notch in all cases.

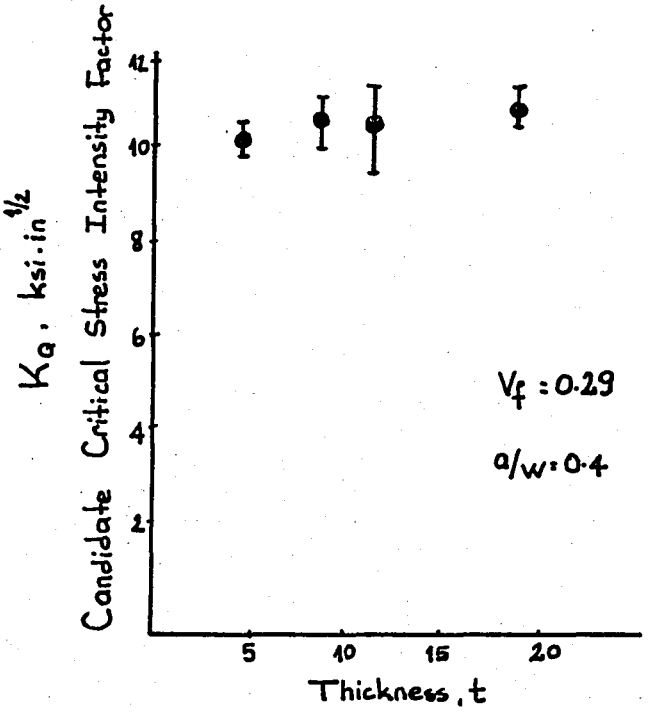

FIGURE 2.7 Variation of K_Q with specimen thickness for the brittle composite [4]

III. APPLICABILITY OF LEFM TO RANDOMLY ORIENTED GLASS FIBER REINFORCED COMPOSITES

3.1 THEORY OF FRACTURE MECHANICS

The recent development of fracture mechanics has shown that there are three primary factors that control the susceptibility of a structure to brittle fracture. [14,15]

a). Material Toughness; K_{IC}, K_C

Material toughness can be defined as the ability to carry load or deform plastically in the presence of a notch and can be described in terms of the critical-stress-intensity factor under conditions of plane stress, K_C, or plane strain, K_{IC}, for slow loading and linear elastic behavior.

b). Crack Size; a

Brittle fractures initiate from discontinuities of various kinds. These discontinuities can vary from extremely small cracks to much larger fatigue cracks. Although good fabrication practice and inspection can minimize the original size and number of cracks, structures without discontinuities can not be manufactured. Even though only "small" discontinuities may be present initially, these discontinuities can grow by fatigue

to a critical size.

c). Stress Level,σ

Tensile stresses (nominal, residual or both) are necessary for brittle fractures to occur. These stresses are determined by conventional stress analysis techniques for particular structures.

The recent development of fracture mechanics as an applied science has shown that all three of the above factors can be interrelated to predict the susceptibility of various structures to brittle fracture. Fracture mechanics is a method of characterizing fracture behavior in structural parameters familiar to the engineer, namely, stress and crack size.

Linear-Elastic Fracture Mechanics (LEFM) technology is based on an analytical procedure that relates the stress field magnitude and distribution in the vicinity of a crack tip to the nominal stress applied to the structure, to the size, shape, and orientiation of the crack or crack-like discontinuity and to the material properties.

The stress-field equation (1) show that the distribution of the elastic-stress field in the vicinity of the crack tip is invariant in all structural components subjected to this type of deformation and that the magnitude of the elastic stress field can be described by a single parameter, K_I, designated the stress-intensity factor. (Figure 3.1)

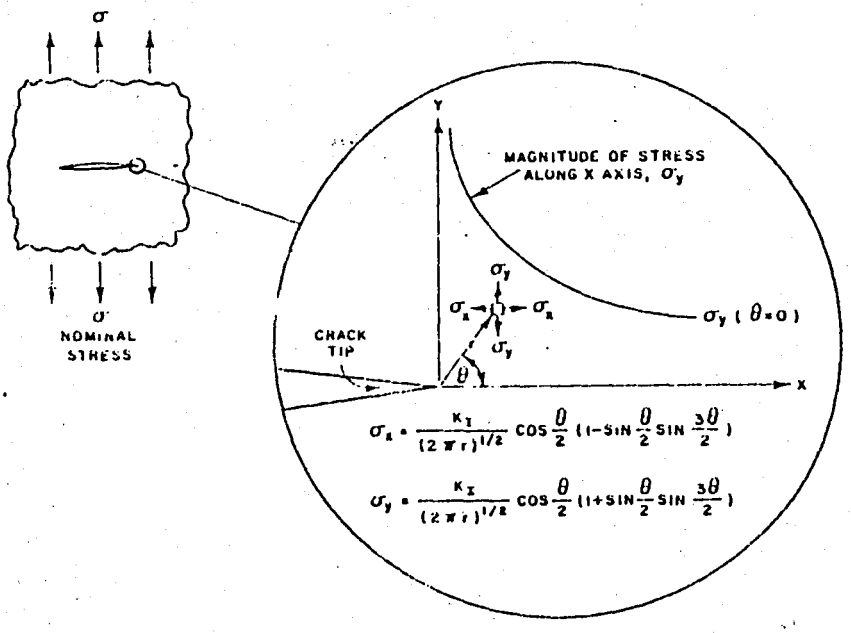

FIGURE 3.1 Elastic-Stress-field distribution ahead of a crack.

$$\sigma_x = \frac{K_I}{(2\pi r)^{1/2}} \cos\frac{\theta}{2}\left(1 - \sin\frac{\theta}{2}\sin\frac{3\theta}{2}\right) + \ldots.$$

$$\sigma_y = \frac{K_I}{(2\pi r)^{1/2}} \cos\frac{\theta}{2}\left(1 + \sin\frac{\theta}{2}\sin\frac{3\theta}{2}\right) + \ldots. \qquad (1)$$

$$\tau_{xy} = \frac{K_I}{(2\pi r)^{1/2}} \sin\frac{\theta}{2}\cos\frac{\theta}{2}\cos\frac{3\theta}{2} + \ldots.$$

Consequently, the applied stress, crack shape, size and the orientiation, and the structural configuration affect the value of the stress-intensity factor but do not alter the stress-field distribution.

One of the underlying principles of fracture mechanics is that unstable fracture occurs when the stress-intensity factor at the crack tip reaches a critical value, K_C.

For mode I deformation, Figure 3.2, and for small crack tip plastic deformation (plane-strain condition), the critical stress-intensity factor for fracture instability is designated K_{IC}.

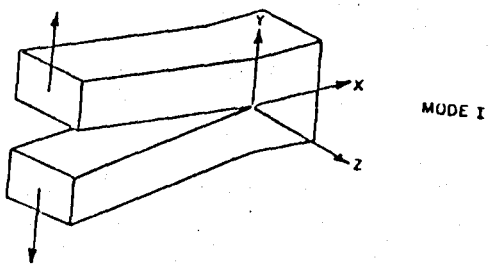

FIGURE 3.2 Configuration of MODE-I loading

K_{IC} represents the inherent ability of a material to withstand a given stress-field intensity at the tip of a crack and to resist progressive tensile crack extension under plane-strain conditions. Thus, K_{IC}, represents the Fracture Toughness of the material.

Dimensional analysis of equations (1) indicates that the stress-intensity factor must be linearly related to stress and must be directly related to the square root of a characteristic length. Based on Griffith's original analysis of glass members with cracks and the subsequent extension of that work to more ductile materials, the characteristic length is the crack length in a structural member.

Consequently, the magnitude of the stress intensity factor must be directly related to the magnitude of the applied nominal stress (σ), and the square root of the crack length(a).

In most cases, the general form of the stress intensity factor is given by

$$K = f(g) \cdot \sigma \cdot \sqrt{\pi a} \qquad (2)$$

where f(g) is a parameter that depends on the specimen and the crack geometry. This parameter was given in appendix-A as a table for single-edge notched (SE(T)) specimens used for this study.

3.2 DETERMINATION OF CANDIDATE CRITICAL STRESS INTENSITY FACTOR, K_Q

Generally, the K_{IC} testing procedure is used for calculating the fracture toughness value for randomly oriented glass fiber reinforced composites. But, two other approaches described in 3.2.2 and 3.2.3 are included in this study as well. Although these approaches are not standard methods it was tought that they could be useful for design purposes.

3.2.1 K_{IC} Testing

The critical stress intensity factor, K_{IC}, testing method to fracture is the method which is most widely used for metallic materials and has therefore been the approach which most workers have attempted to apply to composite materials. The method predicts the onset of crack propagation when the elastic stress distribution around the crack tip reaches a critical level characterized by the Critical stress intensity factor (K_{IC}).

For brittle materials K_{IC} is found to be independent of crack length and is therefore regarded as a material constant

If the material is more ductile the stress intensity approach is still found to be valid provided a correction is made for the region around the crack tip where the stress exceeds the yield stress of the material. It is limited to small scale yielding range, however the correction due to Irwin plastic zone is made by adding an amount to the crack length at failure given by equation (3) [4]

$$r_y = A \left(\frac{K}{\sigma_{ys}}\right)^2 \qquad (3)$$

where $A = \frac{1}{2}\pi$ for plane stress and $\frac{1}{6}\pi$ for plane strain conditions, and K is the stress intensity factor, σ_y is the yield stress of the material.

For the randomly oriented glass fiber reinforced polyster composites, a sharp notch root can not be produced as in the case of metals, thus a small scale plastic zone or in other words, a damage zone is seen at the notch tip in tension. Damage or debonding zone of the composite will be given in detail in section 4. In calculations, total crack length containing the debonding zone ahead of the crack tip was determined by using Crack detection compliance curve.

As there is no standard procedure for K_{IC} testing for the randomly oriented short-glass-fiber reinforced composites, the ASTM standard method proposed by Brown and Srawley for plane strain testing has been implemented where possible to analyse the data obtained.

This method uses load vs. displacement curve. To obtain K_{IC} values from these curves, the ASTM standard method (E-399-74)

suggests that the initial slope Mo of the curve should be obtained and a line of slope 5 percent less than Mo be drawn. (Figure 3.3). This line intersects the curve at a load termed P_5. The highest load in the test up to and including the P_5 (usually itself) is termed P_Q and is used to calculate the candidate critical stress intensity factor, (K_Q). Provided that certain conditions are satisfied K_Q is then a measure of the plane strain fracture toughness, K_{IC}.

These conditions are :

$a > 2.5\ (K_{IC}/\sigma_D)$

$t > 2.5\ (K_{IC}/\sigma_D)$

$w > 5.0\ (K_{IC}/\sigma_D)$

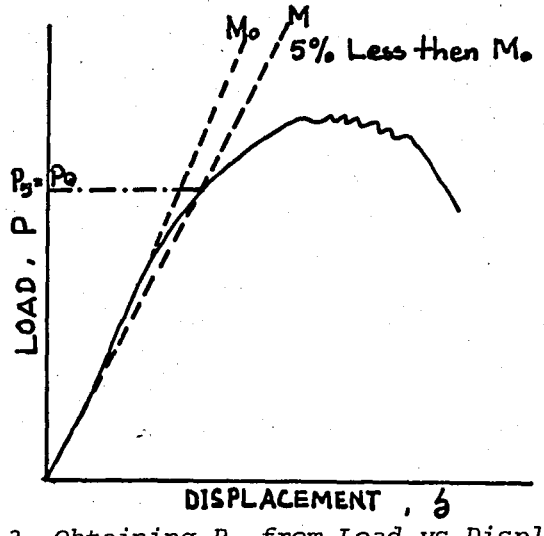

FIGURE 3.3 Obtaining P_Q from Load vs Displacement Plot.

3.2.2 Unstable Crack Propagation Approach

In this approach the stress is calculated by using the load at which unstable crack propagation occurs and then this stress is substituted into equation 2. to calculate a critical stress intensity factor (Figure 3.4)

This approach, although used by some researchers[5,6,11] is not standardized and the stress intensity value obtained can not be termed as a material property (fracture toughness) Furthermore, the stress intensity value thus obtained is not conservative. However, it is easy to determine this value by use of the load-displacement curve and it mihgt be used in some design applications if incorporated with a safety factor.

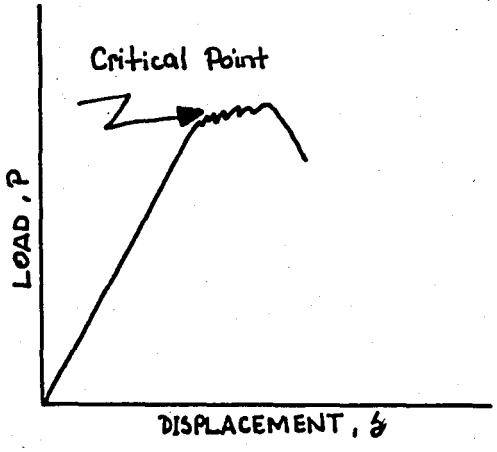

FIGURE 3.4 Determination P_{cr} from critical point.

3.2.3 Debonding Point Approach.

Since the critical stress intensity factor should correspond to the crack initiation point, it can be argued that K_Q should be based on the load corresponding to the onset of debonding in the material.

If the stress intensity factor corresponding to debonding is denoted by K_D, its value can be calculated by substituting 65 percent of the maximum load in the appropriate K-equation-2 (This load being the load at which debonding starts has been verified in this study by observations through the travelling microscope)

Gaggar and Broutman [3] have found that K_D values were lower than the K_Q values for random-glass fiber epoxy composites. The more conservative K_D values may be more appropriate if used in design applications. It is again useful to note that this approach as well as the above discussed unstable crack propagation point approach is of speculative interest as yet.

IV. CRACK TIP RADIUS AND DAMAGE AT A CRACK TIP

4.1 THE VARIATION OF TENSILE STRENGTH AND WORK OF FRACTURE WITH NOTCH ROOT GEOMETRY

Although the correlation of notch root radius with tensile strength and work of fracture does not exactly explain the variation of fracture toughness of randomly oriented short glass fiber reinforced composites with notch root radius, it is useful in that it gives us an idea of how this variation might be.

Table 4.1 shows the effect of the notch root geometry on the tensile strengths of polycarbonate (PC) and randomly oriented glass fiber reinforced polycarbonate. The sharp 60^{o} notch decreases the tensile strength of unnotched polycarbonate to 40 percent. Rounding of the 60^{o} notch base with a 1.5mm radius improves the tensile strength to 90 percent of that of the unnotched specimen [16]. (Figure 4.1)

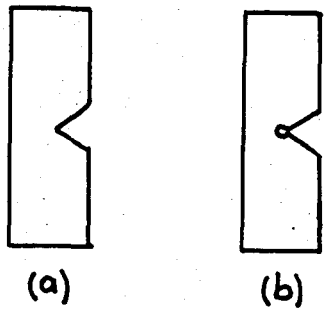

FIGURE 4.1 Sharp(a) and dull(b) notches of specimens of PC. (Polycarbonate)

TABLE 4.1 Effect of Notch Geometry on Tensile Strength [16]

Material	Tensile strength kg/mm^2	
	(a)	(b)
Polycarbonate	2.7(0.40)	6.1(0.91)
Reinforced Polycarbonate	3.6(0.34)	4.4(0.42)

*Value in parantheses indicates the ratio of σ_f to a unnotched specimen

Figure 4.2 shows that the measured work of fracture of carbon fiber reinforced polyster decreases with decreasing notch root radius. [17] The effect is a relatively minor one. The sharper the notch, the greater the stress concentration and the lower the energy input necessary to propagate the crack.

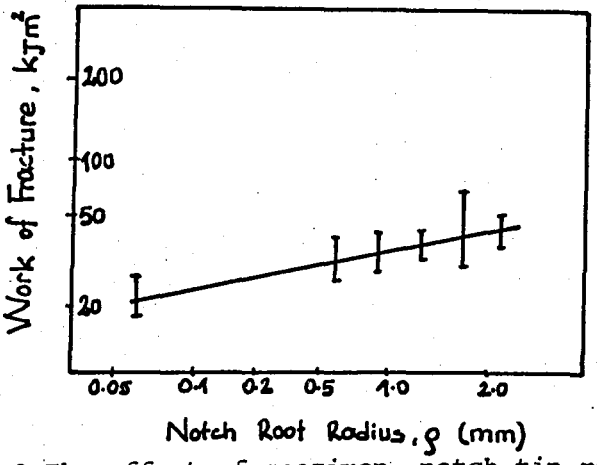

FIGURE 4.2 The effect of specimen notch tip radius on measured work of fracture values for unidirectionally reinforced carbon fiber/ epoxy composites [17]

4.2 DAMAGE ZONE AT THE CRACK TIP

4.2.1 The Development of a Damage Zone During Monotonic Loading.

For many fiber composites, the debonding energy and pull-out energy are the most dominant energy absorption mechanisms responsible for imparting the high fracture energies to such systems. The debonding mechanism is thought to be more important for randomly oriented short glass fiber reinforced resin composites, and the development of a debonded zone at a crack tip has been observed by various investigators [2,5,6,7,18]

The debonding at the crack tip in the composite is analogous to the process of the plastic zone development in the plastically deformable materials. The plastic zone size depends on the type of stress state at the crack tip and the expressions for such a zone at the crack tip under plane stress and plane strain conditions are as in equation (3). Randomly oriented glass fiber-resin composites do not yield but instead debonding between the fiber and matrix, where the fibers are perpendicular to the line of load, can occur. With increasing load the damage is intensified until complete seperation of the specimens occurs.

Sence these composites are isotropic, the expressions for plastic zone size can be modified by replacing σ_y with the debonding stress σ_D, which can be defined as the ciritical stress value at which debonding is initiated in the material under a uniaxial tensile load.

For random glass fiber composites, the plastic zone size expressions can be modified and rewritten as follows,

$$r_D = \left(\frac{1}{2\pi}\right) \left(\frac{K_D}{\sigma_D}\right)^2 \text{ for plane stress} \qquad (4)$$

$$r_D = \left(\frac{1}{6\pi}\right) \left(\frac{K_D}{\sigma_D}\right) \text{ for plane strain} \qquad (5)$$

where r_D is the debonded zone size at the crack tip [18]. Using the above equations, it is thus possible to predict the debonded zone for planar isotropic composites if σ_D for the material can be determined.

Experimentally observed and theoretically calculated values of the debonded zone size are quite close to each other for plane strain conditions [18]. This is not surprising because the stress state at the crack tip may be closer to the plane strain conditions due to the fact that the fibers provide constraints to the matrix material in the transverse direction and hence a tri-axial state of stress exists near the crack tip, independent of the thickness of the composite.

These indicate that the debonded zone size is not small compared to the initial crack length and the effect of the debonded zone should be included in calculations of the fracture parameters. For that reason, this effect was included in this study in the calculation of K_{IC} by means of crack detection compliance curve which gives the equivalent amount of slow crack extension or notch producing the same compliance.

4.2.2 The Development of a Damage Zone During Cyclic Loading

During cyclic loading the material's response to tension clearly changes with the number of cycles and becomes less resistant to the applied stress. [19,20] Changes in shape and size of hyterisis loops during cyclic loading indicate an increase in thermodynamically irreversible damage in the material. The extent and shape of this damage is generally affected by loading variables (e.g., the maximum fatigue stress,the cyclic stress amplitude, loading frequency), material properties (e.g., fiber and filler volume fractions, fiber orientation distribution, dispersion of fibers and filler etc.), geometric parameters (e.g., notch root radius, holes,boundaries, and other cut-outs) and environmental conditions (e.g., temperature, moisture, etc) [21,22]

Direct consequences of the fatigue damage are, decrease of structural integrity and destruction of load transfer mechanisms in the composite. Considering this feature, when the material is subjected to cyclic loading with a peak load equal to its debonding load (65% of the fracture load) the following situations occur.

The size of the hysterisis loop of the first load excursion is much larger than the next ones due to growth of existing notch and initiation of a large number of microcracks.Subsequent cyclic loading initiates further microdamage and propagates existing cracks but with a decreasing rate. This further development of homogeneous damage is reflected by a continuous decrease in stiffness of the composite and by an increase in

size of the hysterisis loops (Figure 4.3).

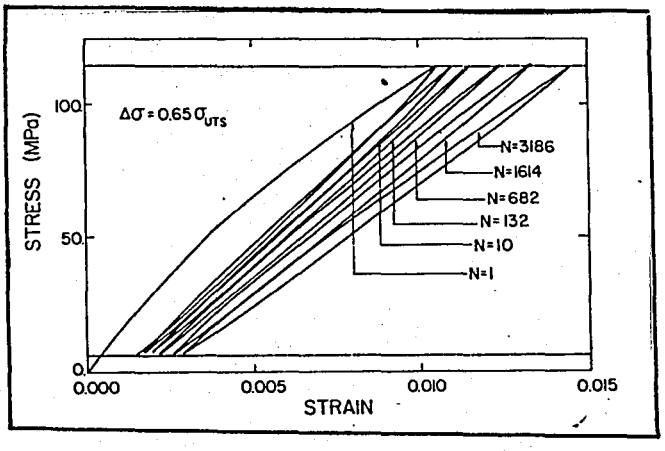

FIGURE 4.3 Stress-controlled fatigue response of the random-fiber-glass reinforced composites [21]

The commonly observed cyclic stable state in metals and polymers is never reached in these types of composite materials [22] The stress-strain curve at any given cycle can be obtained by translating the hysterisis loop at that cycle to the origin. [21-22]. Hence, the cyclic stress-strain behavior of the composite may be expressed by a family of curves at different loading cycles as shown in Figure 4.4

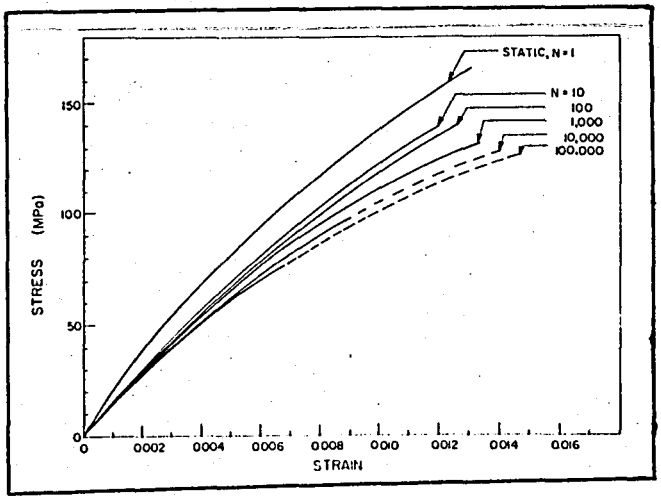

FIGURE 4.4 Monotonic and cyclic stress-strain curves of different loading cycles of randomly oriented glass fiber reinforced polyster (V_f=0.5) [21]

where the first cycle or monotonic stress strain curve is also given for comparison.

In calculating the fracture toughness of a specimen subjected to a certain number of cyclic loading, the effective crack length should be calculated by taking into account the damage produced during fatigue.

V. EXPERIMENTAL WORK

5.1 TEST MATERIAL

The material which is used in the experimental study is a sheet containing chopped glass fiber strands randomly oriented in the plane of the sheet as reinforcement and polyester as matrix.

Polyster used as a matrix is Neoxil 188N8 and glass fiber reinforcement mat is E-type, G11. They are both supplied from Cam Elyaf Sanayi A.Ş. Laminates 530x690 mm are prepared in a temperature - and humidity-controlled laboratory by the wet Lay-Up technique and are allowed to gel for 48 hrs at room temperature before being post-cured for 3hrs at $80^{o}C$.

Generally , Plastics or Polysters used here are of the thermosetting type. (Neoxil 188N8). Thermosets are plastics which are formed once by heating and then which can not be reformed again. Unsaturated Polyster Resin is the most used type polyster. Its mechanical, chemical and electrical properties and easy usabilities enable it to be used extensively according to aim of application and design point of view (Table 5.1)

TABLE 5.1 The Properties of a Cured Polyster

Specific Density	1.15-1.25
Elastic Modulus	3000-4000 N/mm^2
Tensile Strength	50-80 N/mm^2
Bending Strength	30-130 N/mm^2
Deformation Temperature Under Loading	50-150 ^oC
Hardness (Barcol)	$\sim$ 50

Ortophtalic Polyster Resin

Glass mat , Gll specially, is produced as in the Figure 5.1

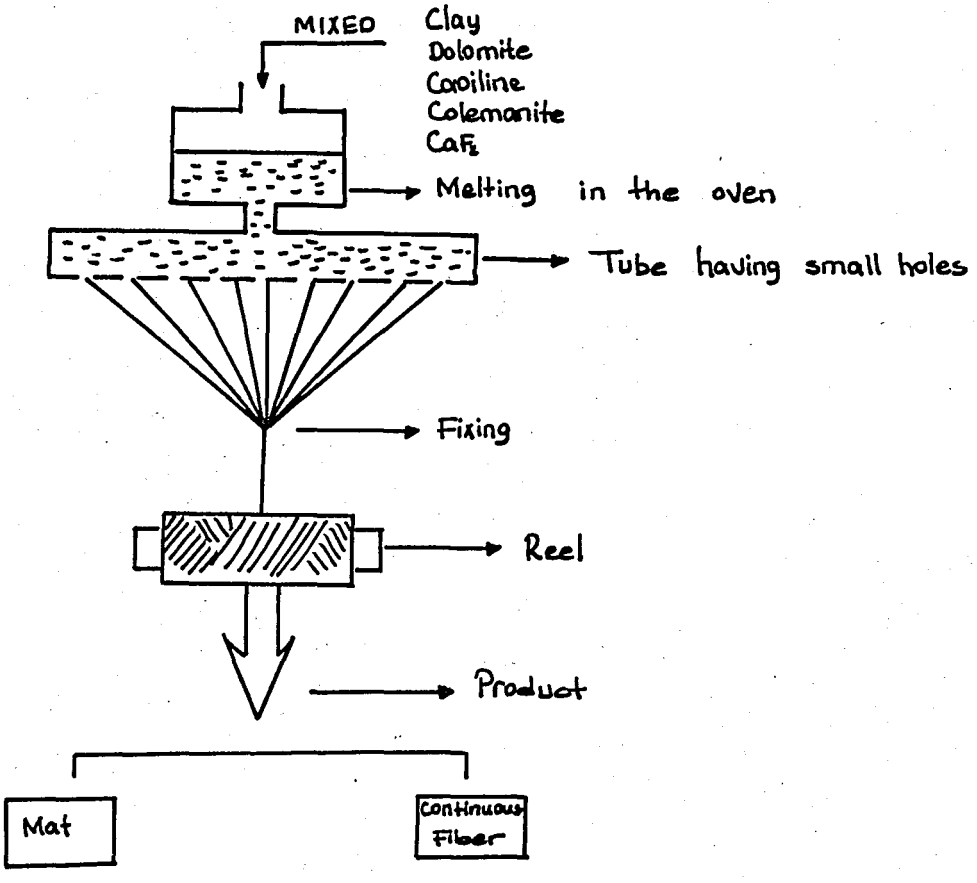

FIGURE 5.1 A configuration of the glass fiber producing method.

For producing wide plates, for example a truck cabin, the LAY-UP method is used extensively. A convenient die remover is first spread and polished. After that, the polyster resin is applied to the surface once or twice with a roller. Then the glass mat is spread in one layer or more, it is saturated with polyster completely and rolled until the glass mat is wetted. Finally, it is left to be cured at room tempetarure. (Figure 5.2)

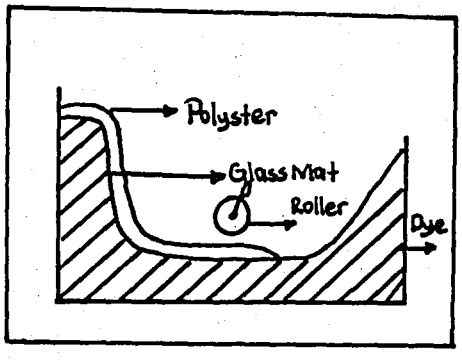

FIGURE 5.2 Producing wide plates

The chemical composition of the composite used here is given in table 5.2.

TABLE 5.2 The chemical composition of the composite

Reinforcement	Type	Weight %
	Etype,G11	32.8
Matrix	Neoxil 188N8	67.2

5.2 SPECIMEN GEOMETRY

Tensile testing and fatigue testing specimens were chosen according to ASTM 3039-74D. Single Edge Notched in Tension (SE(T)) specimens as shown in figure 5.3(a) are generally convenient for sheet materials. They are used for mode-I fracture and fatigue tests.

All specimens are cut from the sheets and milled to the dimensions required. The specimens have a length of 300 mm and a width of 50 mm. The total gage length between grips is 178mm. They are heated to 80^{o}C for 3 hrs as a post-cure with tabs and furnace cooled at the rate of 0.1 C^{o}/min. (Table 5.3)

After heat treatment, specimens are notched at the same length and various notch root radii with a thin circular slitting saw. The sharp notches whose root radius g<0.25 mm are achieved by cutting slowly to the depth required with a very thin saw and by finishing to the desired notch root radius with a knife having sharp edges (0.125 mm in thick). The others are drilled with various drills. When obtanining blunter notches, holes are drilled first through the specimen and a fine saw used to cut through from the edge of the specimen to the hole.

The notch root radius and length are measured with a sensitive vernier calipher. The notch root radii are varied from 0.125 mm (sharp) to 2.5 mm and the notch depths are kept constant at a/w=0.3. The notch depths are about 15 mm. with a deviation of $\bar{+}$0.6 mm.

The single edge notched tension specimen (SE(T)) is gripped using parallel-sided strips, namely tabs, made of GRP or

soft aluminium bonded onto the samples. But, GRP (glass reinforced plastics) tabs of the same material as the specimens are preferred due to the good adhesion achieved. They are bonded to the specimens with a commercial adhesive, "404-çelik plastik".

The specimen geometry used for unnotched tensile testing and for tensile testing of the matrix material are the same. (Figure 5.3(b) and Table 5.3)

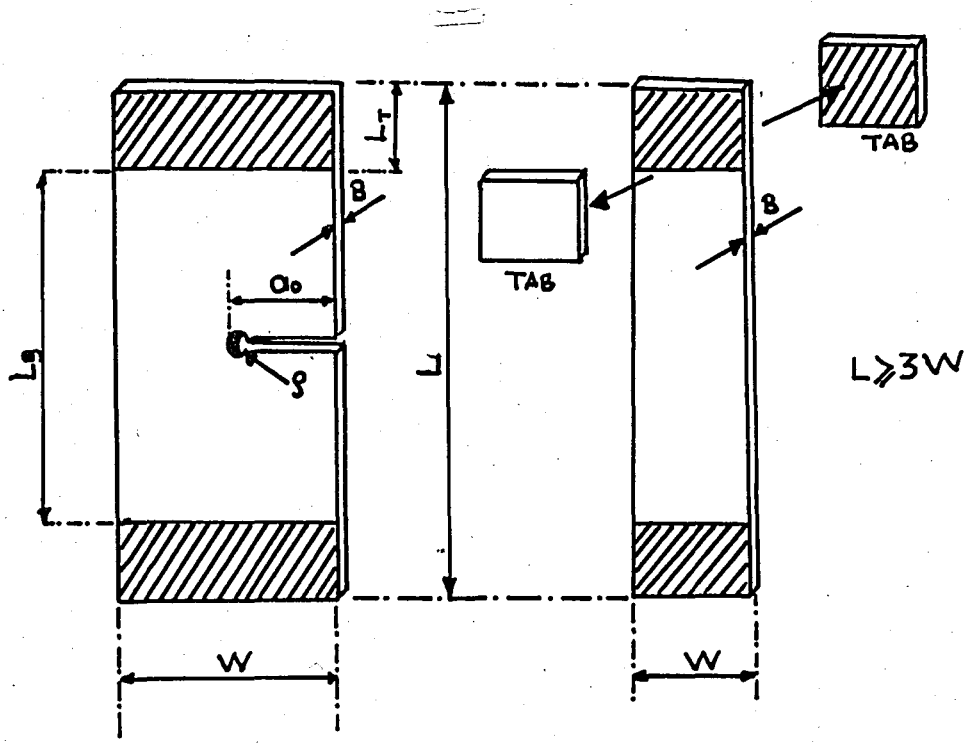

FIGURE 5.3 (a) single-edge-notched specimen (SE(T))
(b) Tension specimen

SE(T) specimen is not only a standard configuration for tension tests but also a common specimen for fatigue and compliance test experiments.

TABLE 5.3 Dimensions of the specimens shown in figure 5.3

	W	a_o	L_g	L	L_{tab}	B
SE(T) SPECIMEN	50	15	178	300	66	3.0-3.5
TENSILE STRENGTH TEST SPECIMENS	25	7.5	178	300	66	3.0-3.5

5.3 SET-UP

All tests are performed on an electro-hydraulic closed loop, MTS 812, fatigue testing machine with a maximum capacity of 10 tons. (Figure 5.4)

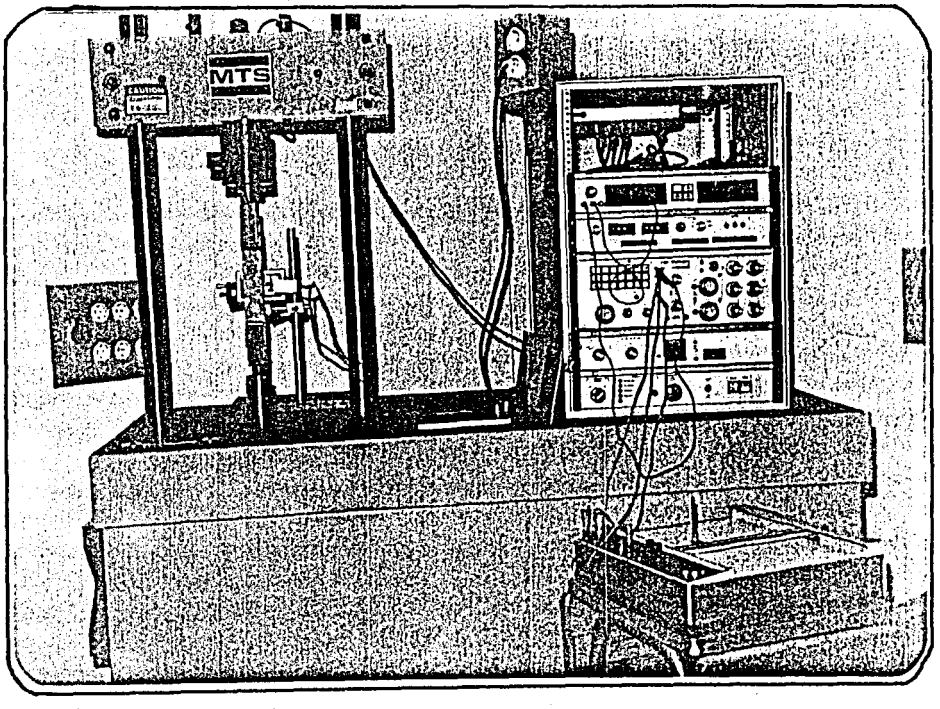

FIGURE 5.4 Fatigue Testing Machine and X-Y Recorder

Tests are conducted under load control. Load and crack mouth displacements are plotted as the ordinate and the abscissa, respectively, on an (Hewlett-Packard) X-Y recorder (Figure 5.4)

The displacement is measured using a clip-gage mounted across the open mouth of the notch. The load is measured through the load cell of the testing unit. The accuracy of the load-cell is ± 1 %.

In order to mount the clipgage on the specimens two knife edges are bonded to the specimens. The schematic of the clip gage and the knife edges used are shown in Figure 5.5

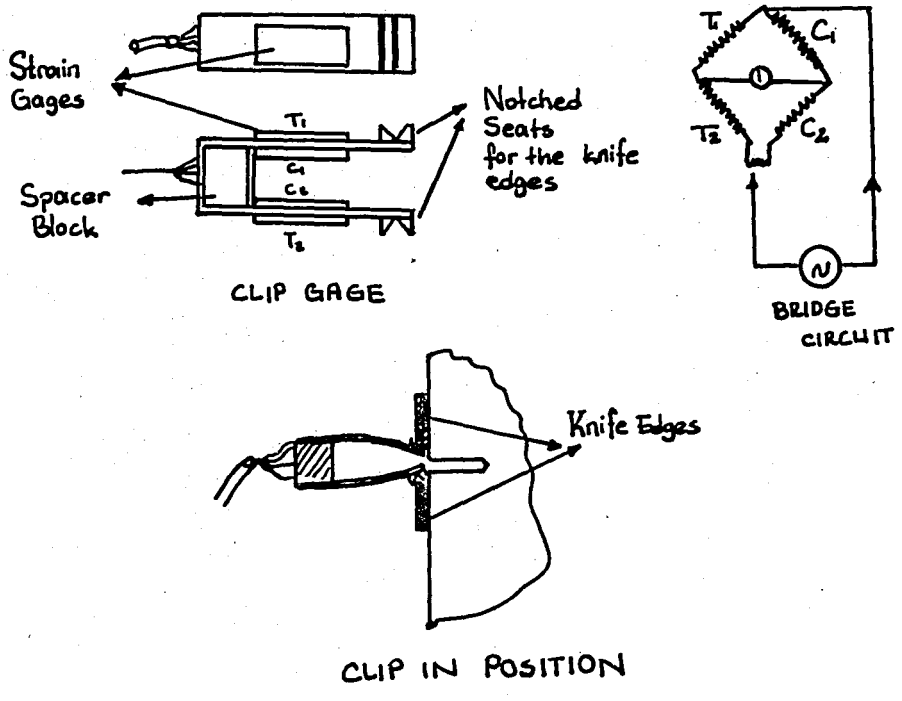

FIGURE 5.5 Schematic of the displacement gage.

Grips were specially designed for thin sheet materials. The small tabs inside the grips were serrated for holding the specimen completely.

5.4 MEASUREMENT OF THE CRACK LENGTH

In static and fatigue loading, diffuculty can be experienced in measuring the crack length due to the damage developed at the tip of the crack. Measurement of the crack length during loading is especially difficult in glass fiber composites because of the two-phase nature of the material and the large amount of irreversible debonding which occurs around the crack tip. Both sih and Thornton [23] (1970) used optical means to measure the crack length but experienced difficulty.

Several methods can be tried out to measure the crack length as a function of damage. These include;

1. Using an optical travelling microscope
2. Using penetrating dyes
3. Using a calibration curve

The method using the travelling microscope is not successful since the crack does not propagate along a neat line as in metals due to the presence of debonding between fibers and the matrix. Use of penetrating dyes is not successful either since the dye may run along surface cracks which indicate erroneously large crack length. Usually, these surface cracks do not extend through the thickness.

The method using extension gage (clip gage) does not

measure the crack length directly, but it is measured by means of the crack detection compliance curve (Figure 5.6) This means that at a specified point on load-displacement curve the compliance corresponding to that point is measured, value of the crack length or damage is then obtained indirectly from the crack-detection compliance curve for every specimen.

5.4.1 Construction of Crack Detection Compliance Curve

As known, compliance is defined as

$$C = \frac{\delta}{p} \qquad (6)$$

where δ is the crack-mouth displacement and p is the load. It should be pointed out that the machined slot necessary to simulate crack does not provide exactly the same specimen compliance as a natural crack. In this study, the machined crack in the compliance specimens and the fracture test specimens were of the same type, hence it is expected that the compliance specimen will simulate the behavior of the fracture test specimen.

To construct the crack detection compliance curve, the load-displacement records are first obtained for specimens having cracks of various lengths, all produced by increasing the crack length with a Jeweller's saw in 5 mm. increments. Initial straight-line portions of the load / displacement records at various initial notch lengths are used to calculate the compliance. Then the product of compliance and thickness is plotted to various crack lengths to obtain the crack detec-

tion compliance curve. (Figure 5.6). A conventional compliance calibration curve (EBC vs a/w) is also given for general purposes. (Figure 5.7)

The data obtanied from calculations are processed with a computer program using the least-square method to fit the curve to the points (Figure 5.6 and 5.7) The program will be given in the appendix-B

5.5 EXPERIMENTAL PROCEDURE

Since this study tries to investigate the effect of notch root radius on fracture behavior and the effect of fatigue (cyclic stress) on fracture toughness, experiments are divided into three sections.

(a) Construction of crack detection Compliance Curve

(b) Static fracture tests (monotonic)

(c) Fatigue fracture tests (cyclic)

Before starting the experiment, the machine is prepared for the test. The first three specimens are tested to obtain the crack detection compliance curve; each one is subjected to the tensile loading at the same loading rate at various crack lengths; and for each crack length , load-displacement curve is plotted by loading and unloading without causing debonding at the crack tip. Then, compliances corresponding to the crack lengths are determined. After the three specimens are tested,the crack detection compliance curve is plotted.

Next, specimens with the same crack lengths (a_o=15$\pm$0.6mm)

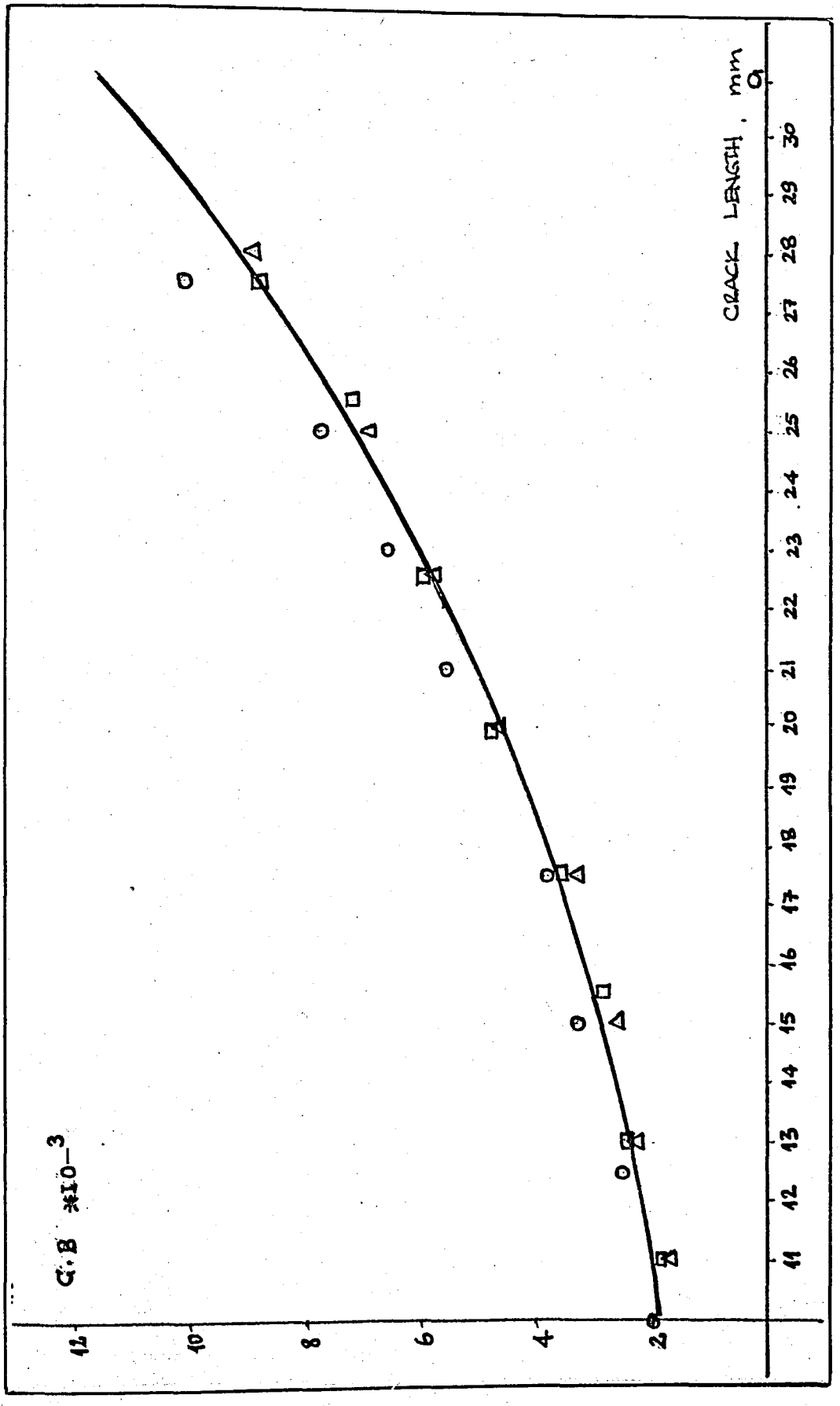

Figure5 5.6 CRACK DETECTION COMPLIANCE CURVE

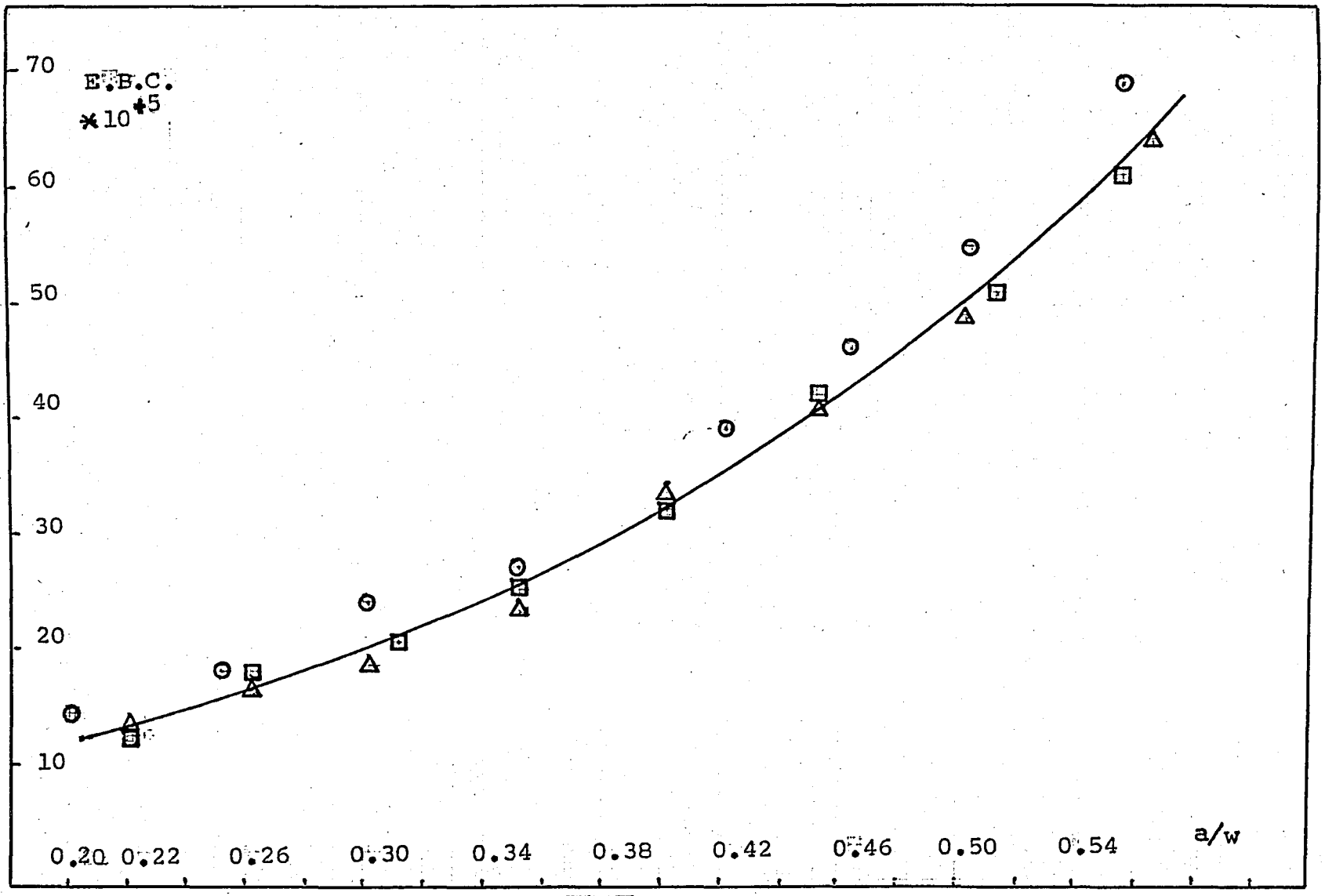

Figure 5.7 COMPLIANCE CALIBRATION CURVE

but different notch tip radii are pulled to fracture. At the same time, load-displacement curves are obtained from the X-Y recorder. For each crack tip radius, three specimens are subjected to testing and their load displacement curves are used to calculate the candidate critical stress intensity factor (fracture toughness) with different methods mentioned section III.

Finally, specimens with the same crack lengths but different notch tip radii are stress-cycled in tension (opening mode) at a rate of 5 Hz. The loading history is of a ramp function varying between a minimum load (20 kg) to a maximum positive peak tensile load (270 kg)(Figure 5.8)

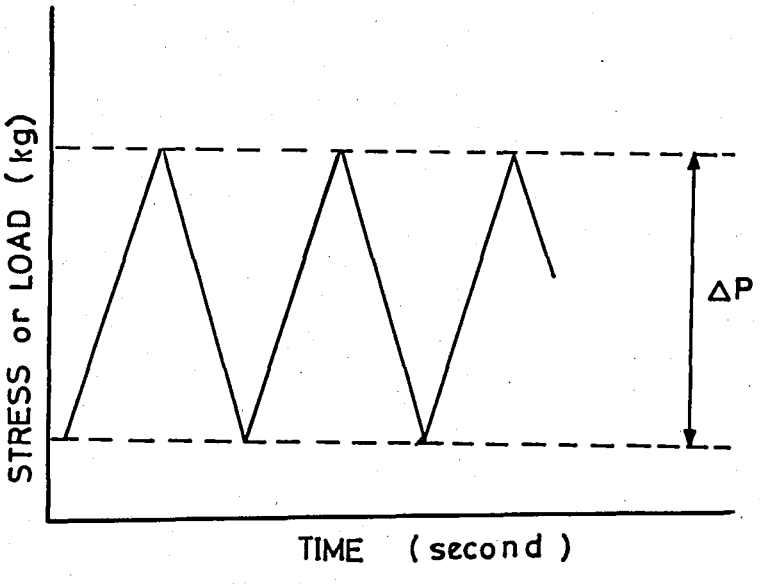

FIGURE 5.8 Cyclic Load function for tensile fatigue

After each specimen has been cycled 10^5 times, they are pulled to fracture at a constant loading rate (reaching to peak load in 200 seconds). The fracture load is recorded and the critical stress intensity factor, K_{IC}, is computed using

the different methods mentioned in section III again.

Results of the notch tip radius and the fatigue on the apparent fracture toughness, K_Q, will be given in the next section. All of these data are associated with specimens which have a crack tip radius varying from 0.125 mm to 2.5 mm

5.6 RESULTS

5.6.1 Static Tensile Testing Results

Figure 5.10 and table 5.4 show the candidate fracture toughness value vs crack tip radius according to K_{IC} testing method.

Figure 5.11 and table 5.5 show the K_I variation with respect to crack tip radius according to unstable crack propagation approach.

Figure 5.12 and table 5.6 show the data obtained according to debonding load with respect to notch tip radius.

5.6.2. Fatigue Tensile Testing Results

Variation of fracture toughness with notch root radius is given in figure 5.13 and in table 5.7 using the K_{IC} procedure of ASTM, in Figure 5.14 and table 5.8 using the unstable point approach and in figure 5.15 and table 5.9 using the debonding approach.

5.6.3 Static Tensile Test Results of Pure Matrix with two Different Notch-Tip Radius

Figure 5.16 gives the variation of fracture toughness with respect to notch-tip radius for the pure polyster resin. (Neoxil 188N8) Only static experiments are performed due to its brittleness. Table 5.10 also gives the data obtained and shows the fracture stress.

A cumulative figure (5.17) is included to show the differences between the virgin and cyclicly loaded specimens.

A typical fracture picture of the specimens is seen in figure 5.9. Other pictures which show the fracture behavior of the specimens with the same crack lengths but different notch tip radii are given in appendix-C.

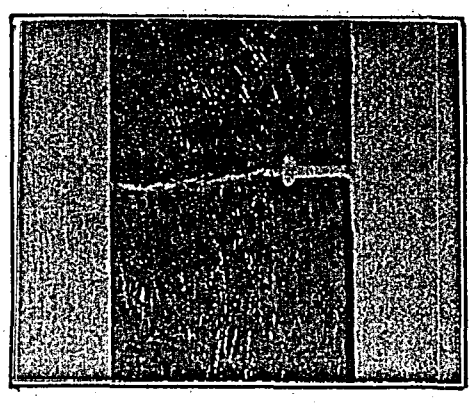

FIGURE 5.9 Fractured specimen with notch root radius of 2.5 mm in static test.

Table-5.4 Stress Intensity Factor Results According To K_{1c} Testing Data (static)

Radius ρ (mm)	Initial crack leng. (a_o)	Final crack leng. (a_f)	Crt. st. int. fct. K_Q
Sharp	15.0	22.6	9.0
Sharp	15.0	15.2	8.71
0.25	14.7	24.8	9.83
0.25	15.6	24.7	10.4
0.5	15.0	21.8	9.86
0.5	15.0	22.6	11.2
0.5	15.2	21.2	11.6
0.75	14.3	26.1	9.48
0.75	14.9	24.4	11.1
1.0	14.9	20.4	10.8
1.0	14.6	26.1	10.6
1.0	15.0	19.8	12.4
1.15	15.0	25.5	10.75
1.15	15.0	23.5	10.56
1.15	14.5	20.9	9.86
2.5	14.8	26.1	9.5
2.5	15.2	22.6	12.5
2.5	15.25	27.0	9.10

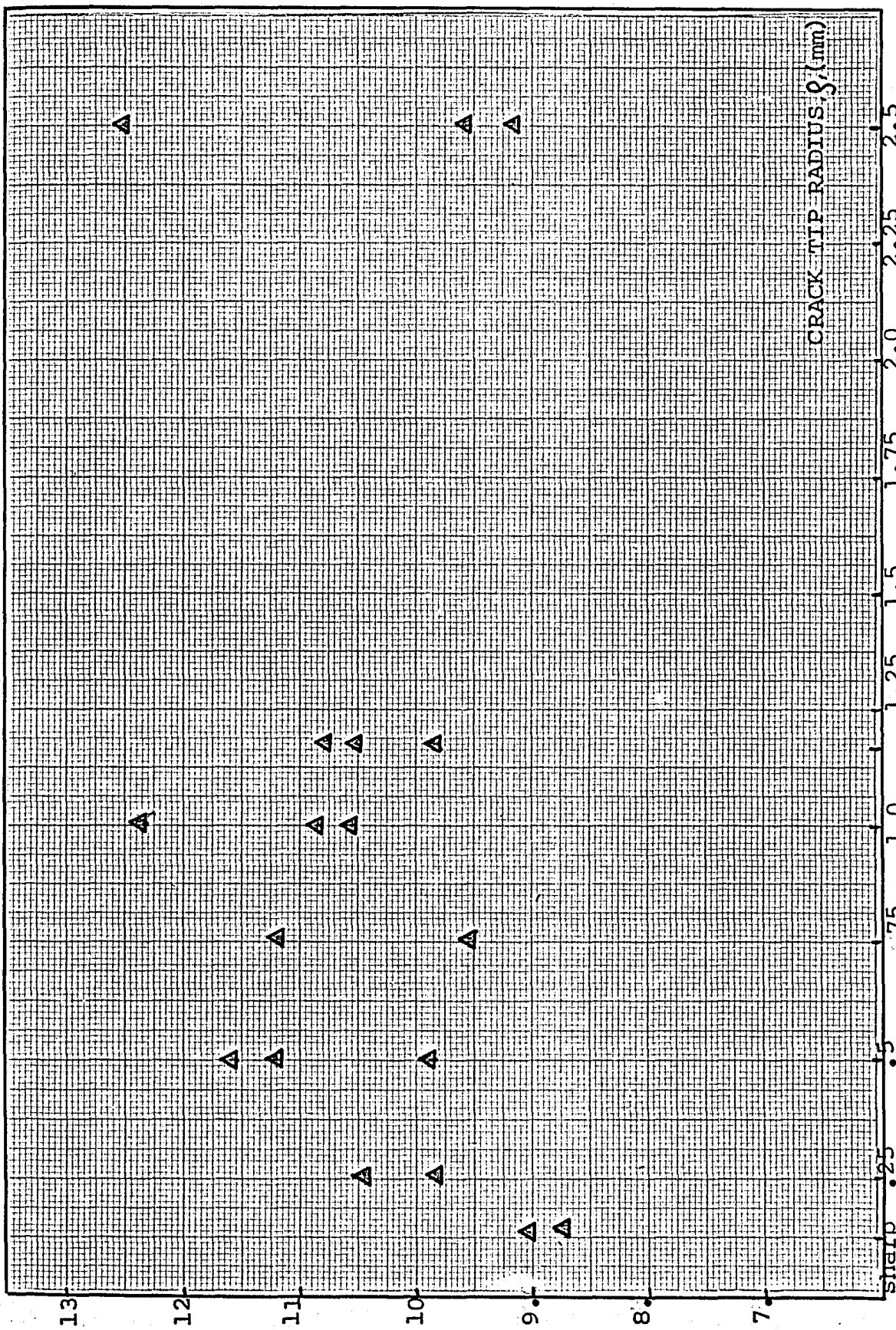

Figure 5.10 Static Tensile Test Result According to K_{1c} Testing Data

Table-5.5 Stress Intensity Factor Results According To UNSTABLE CRCK PROPAGATION Data (static)

Radius ρ (mm)	Initial crack leng. (a_o)	Finalcrack leng. (a_f)	Crt. st. int. fct. K_Q
Sharp	15.0	23.7	11.2
Sharp	15.0	16.8	14.3
0.25	14.7	25.2	14.9
0.25	15.6	26.2	10.7
0.5	15.0	23.7	13.0
0.5	15.0	25.3	14.0
0.5	15.2	22.9	14.8
0.75	14.3	26.8	10.8
0.75	14.9	23.3	11.3
1.0	14.9	23.3	12.8
1.0	14.6	26.6	10.6
1.0	15.0	20.2	15.0
1.15	15.0	27.0	8.02
1.15	15.0	23.6	10.5
1.15	14.5	20.9	10.6
2.5	14.8	27.2	9.95
2.5	15.2	23.5	13.1
2.5	15.25	25.4	9.54

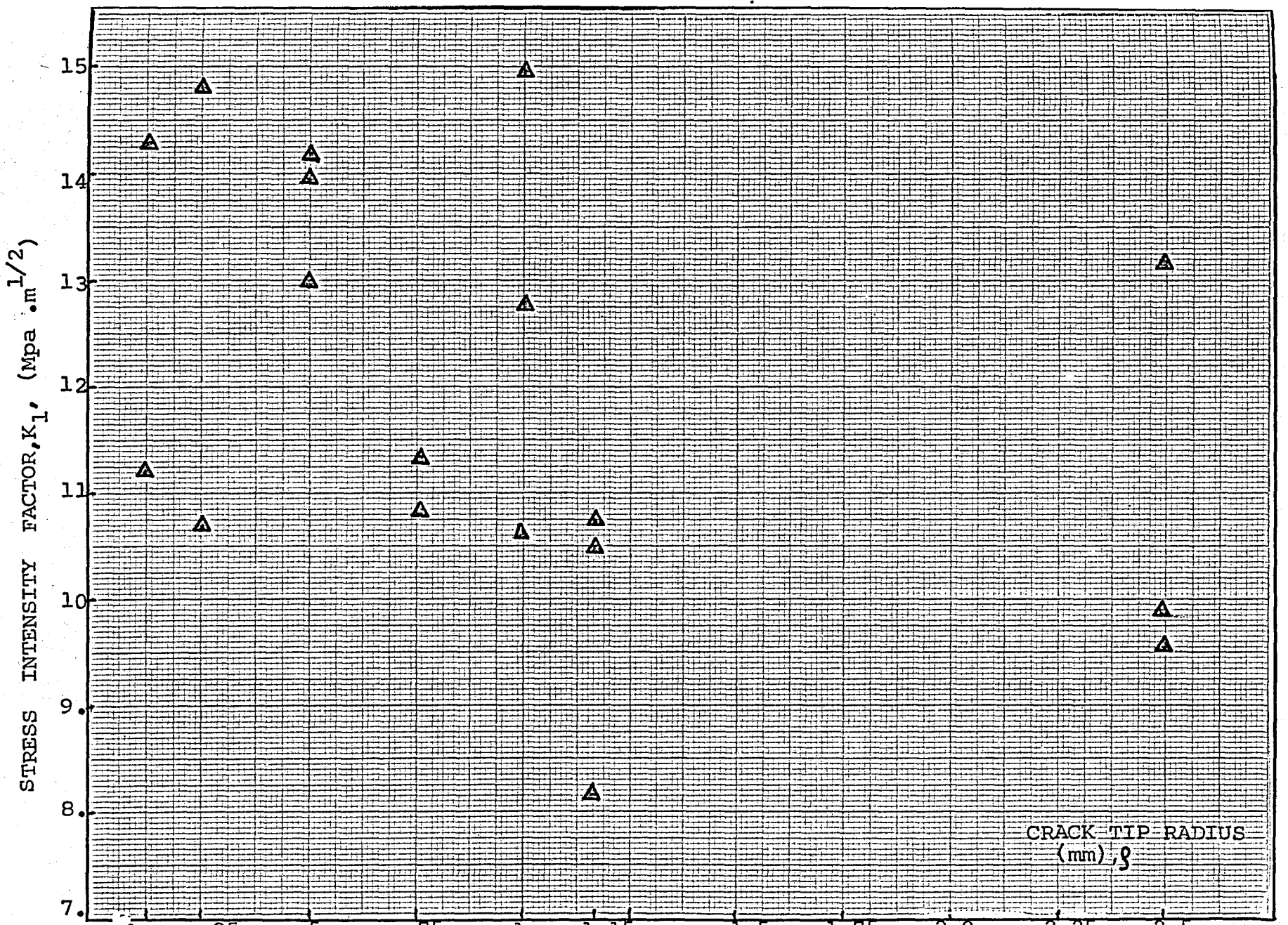

Figure 5.11 Static Tensile Test Result According to Unstable Crack Propagation Data

Table-5.6 Stress Intensity Factor Results According To DEBONDING Point Data (static)

Radius ρ (mm)	Initial crack leng. (a_o)	Finalcrack leng. (a_f)	Crt. st. int. fct. K_Q
Sharp	15.0	22.0	7.78
Sharp	15.0	15.3	9.9
0.25	14.7	18.8	8.46
0.25	15.6	22.7	7.0
0.5	15.0	21.2	8.11
0.5	15.0	23.6	9.11
0.5	16.2	20.2	9.36
0.75	14.3	24.9	7.18
0.75	14.9	22.0	8.0
1.0	14.9	22.2	8.2
1.0	14.6	24.7	7.15
1.0	15.0	19.1	9.93
1.15	15.0	25.5	5.83
1.15	15.0	22.0	7.24
1.15	14.5	19.6	6.91
2.5	14.8	25.0	6.15
2.5	15.2	22.1	8.68
2.5	15.25	25.7	6.38

Figure 5.12 Static Tensile Test Result According to DEBONDING Point Data

Table- 5.7 Stress Intensity Factor Results According To K_{1c} Testing Data (fatigue)

Radius ρ (mm)	Initial (a_o) crack len.	Final crack leng. (a_f)	Crt. st. int. factor K_Q
Sharp	15.5	17.2	7.26
Sharp	15.2	15.4	6.95
Sharp	14.9	15.7	6.08
0.25	15.3	15.9	8.3
0.25	14.6	17.8	8.9
0.25	15.0	15.2	7.31
0.5	14.9	17.4	8.13
0.5	14.8	17.3	10.0
0.5	14.9	16.1	9.6
0.75	15.1	15.4	8.5
0.75	14.3	17.3	8.35
0.75	15.0	15.4	7.75
1.0	14.85	17.5	9.6
1.0	14.6	15.8	8.62
1.0	15.0	17.9	8.82
1.15	15.3	17.1	9.6
1.15	14.5	24.6	9.49
1.15	15.5	18.4	8.73
1.15	14.4	17.2	9.62
2.5	15.0	15.4	9.96
2.5	14.7	14.9	10.37
2.5	15.0	15.2	7.67

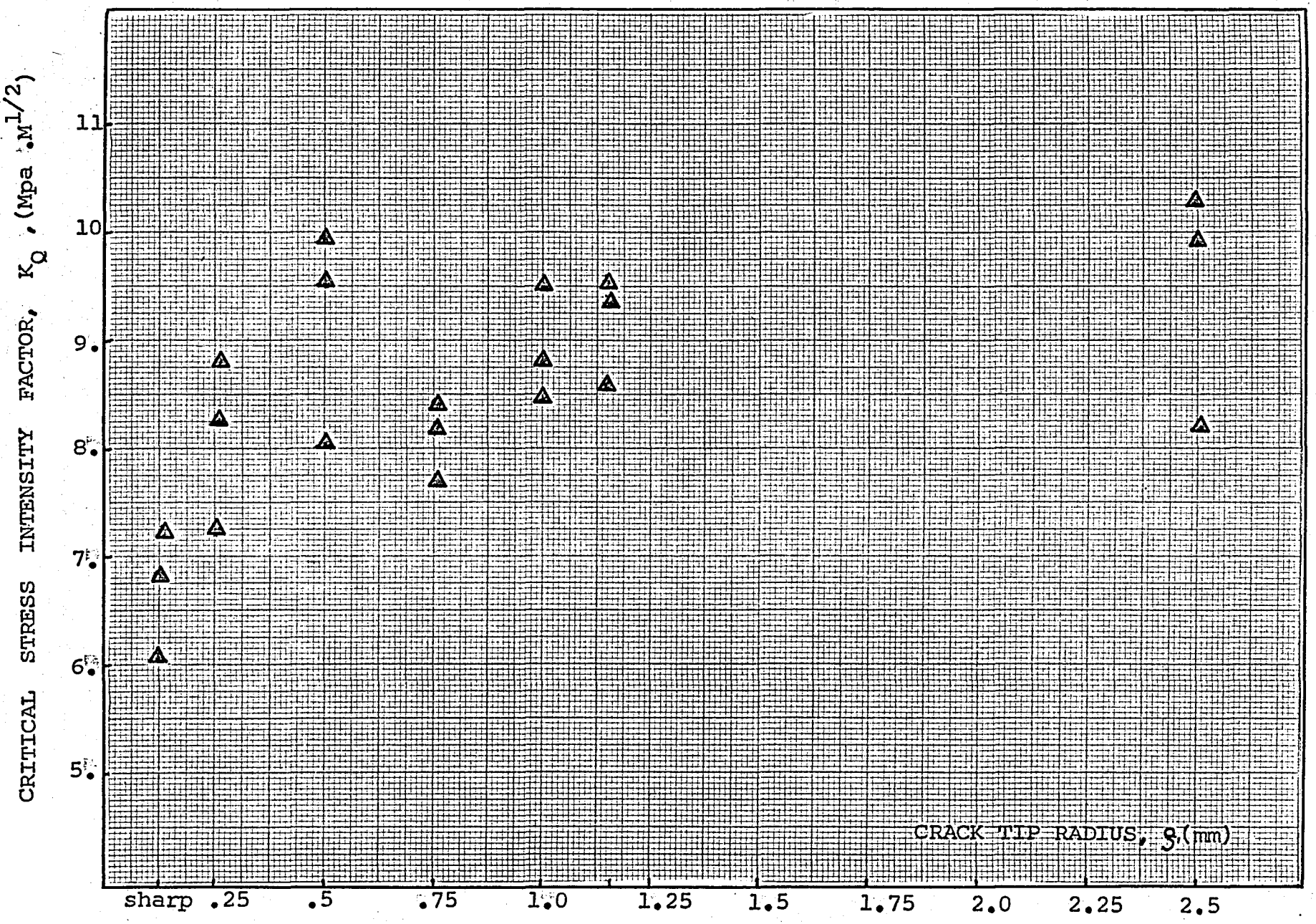

Figure 5.13 Fatigue Tensile Test Result According to K_{1c} Testing Data

Table-5.8 Stress Intensity Factor Results According To UNSTABLE CRACK PROPAGATION Data (fatigue)

Radius ρ (mm)	Initial (a_o) crack len.	Final crack leng. (a_f)	Crt. st. int. factor K_Q
Sharp	15.5	17.5	7.57
Sharp	15.2	16.2	7.56
Sharp	14.9	16.2	6.58
0.25	15.3	18.1	9.33
0.25	14.6	17.6	8.54
0.25	15.0	15.2	7.34
0.5	14.9	18.6	8.56
0.5	14.8	17.5	10.5
0.5	14.9	16.7	12.4
0.75	15.1	15.4	8.5
0.75	14.3	17.9	10.7
0.75	15.0	15.7	9.0
1.0	14.85	18.1	10.18
1.0	15.0	17.9	9.86
1.0	14.6	16.2	9.68
1.15	15.3	17.2	7.6
1.15	14.5	25.0	10.2
1.15	15.5	19.1	9.64
1.15	14.4	17.9	10.4
2.5	15.0	15.4	10.6
2.5	14.7	14.9	10.3
2.5	15.0	21.2	10.3

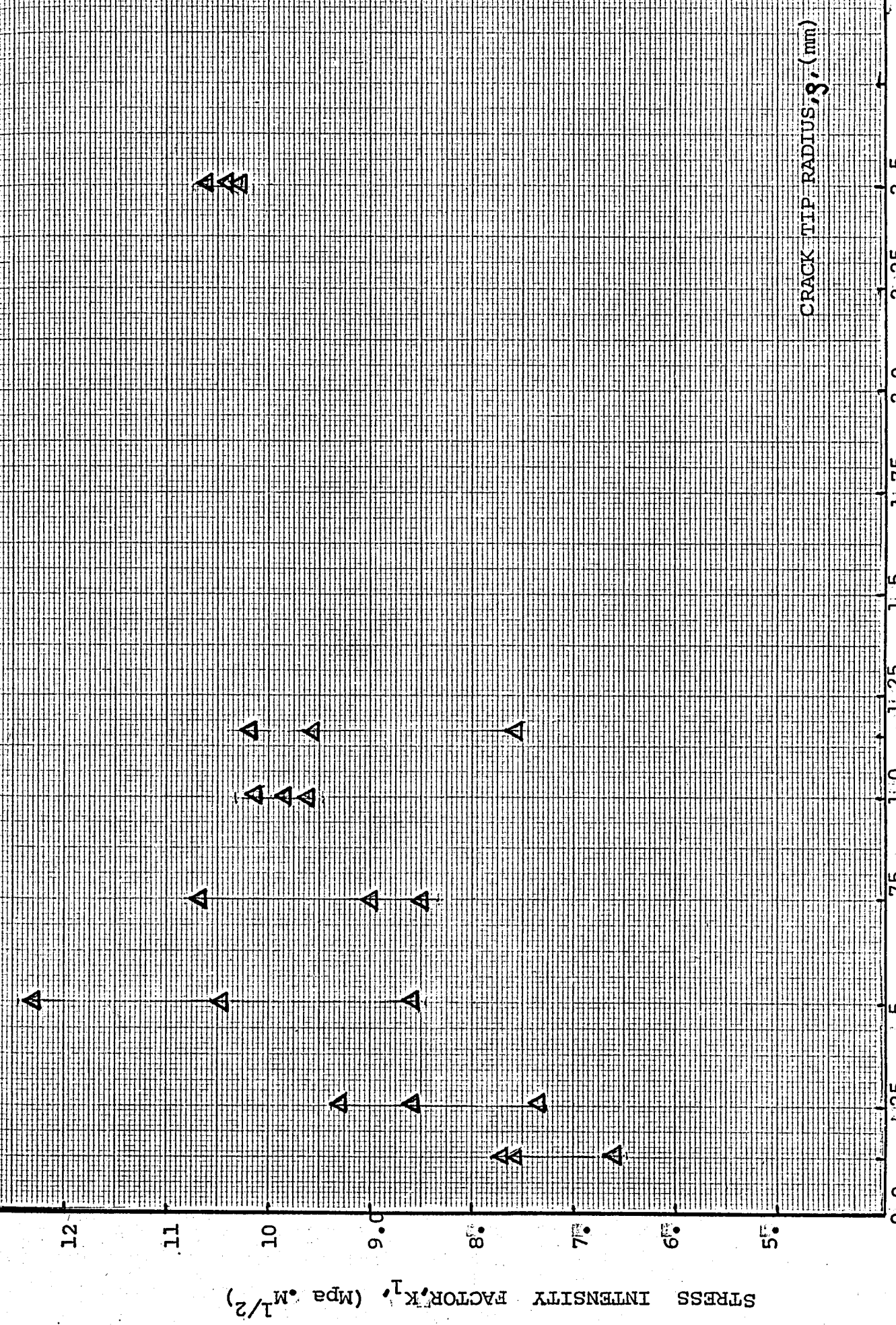

Figure 5.14 Fatigue Tensile Test Result According to UNSTABLE CRACK PROPAGATION Data

Table-5.9 - Stress Intensity factor Results According To DEBONDING Data (fatigue)

Radius ρ (mm)	Initial (a_o) crack len.	Final crack leng. (a_f)	Crt. st. int. factor K_Q
Sharp	15.5	16.2	5.0
Sharp	15.2	15.4	5.7
Sharp	14.9	15.9	4.66
0.25	15.3	17.1	6.38
0.25	14.6	17.6	6.42
0.25	15.0	15.0	5.0
0.5	14.9	16.0	8.58
0.5	14.8	17.0	7.0
0.5	14.9	17.2	5.74
0.75	15.1	15.1	6.44
0.75	14.3	14.9	6.38
0.75	15.0	15.1	6.0
1.0	14.85	17.2	7.5
1.0	14.6	15.0	6.29
1.0	15.0	16.2	6.56
1.15	15.3	16.2	4.8
1.15	14.5	23.3	6.57
1.15	15.5	17.4	6.1
1.15	14.4	17.2	6.9
2.5	15.0	15.8	7.1
2.5	14.7	15.4	6.9
2.5	15.0	15.1	7.0

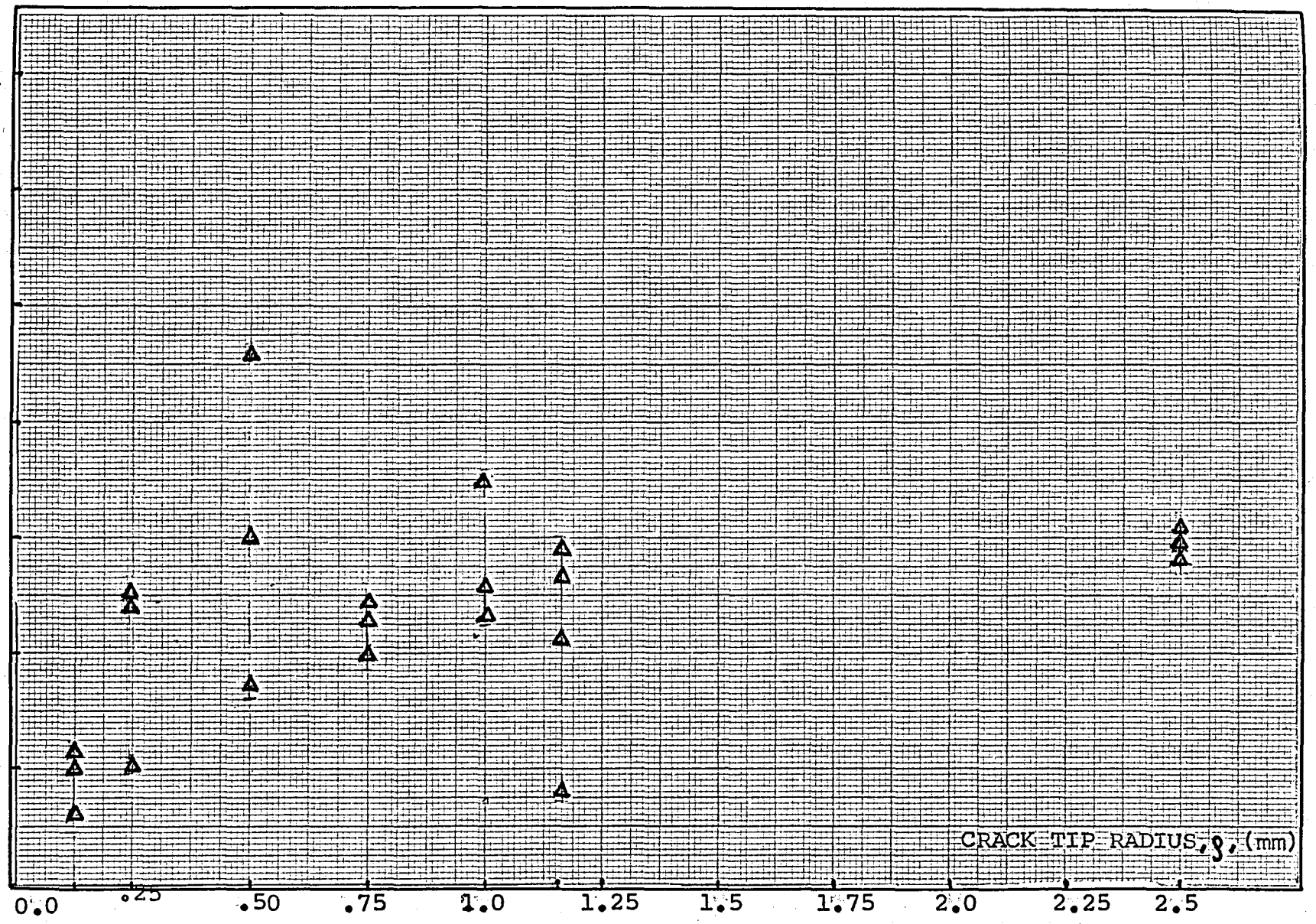

Figure 5.15 Fatigue Tensile Test Result According to DEBONDING point Data

Table-5.10 Pure Matrix Data With Two Different Crack Tip Radius. (Static Tensile Test Data)

RADIUS (mm)	σ_f (Mpa)	K_{1c}
Sharp	6.17	1.63
Sharp	7.38	1.98
Sharp	9.48	2.38
Sharp	9.12	2.43
1.0	16.0	4.0
1.0	12.5	3.22
1.0	13.2	3.44

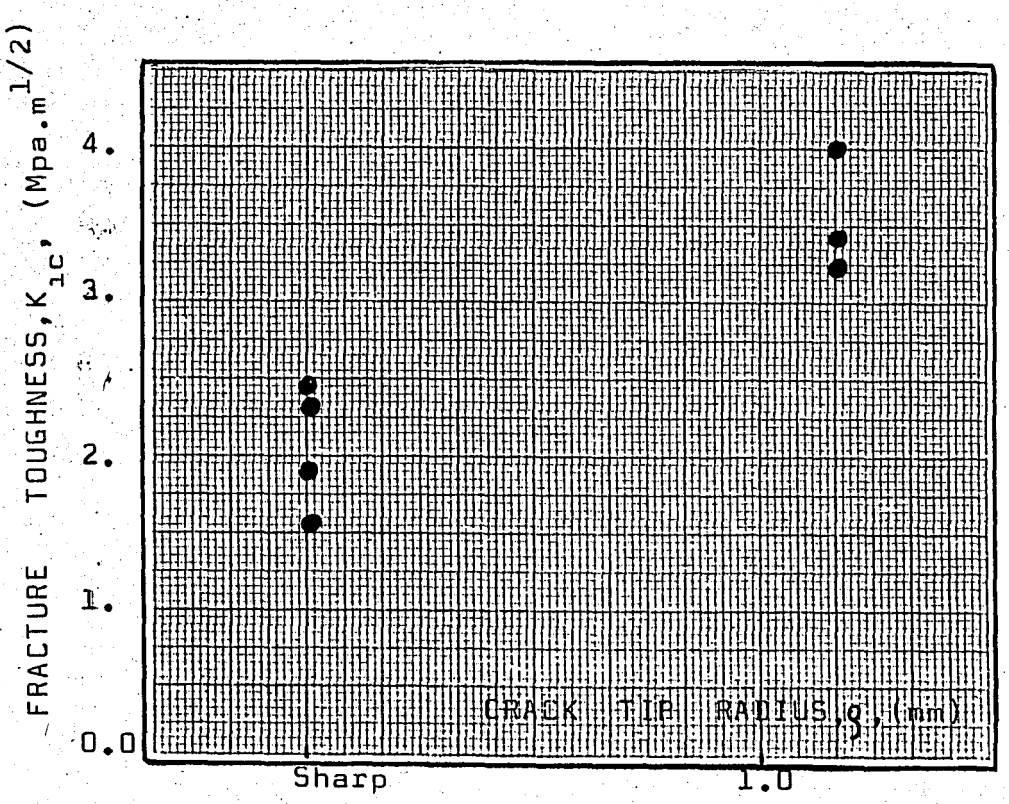

Figure-5.16 Static Tensile Test Data With Various Crack Tip Radii Of Pure Matrix(neoxil 108p8)

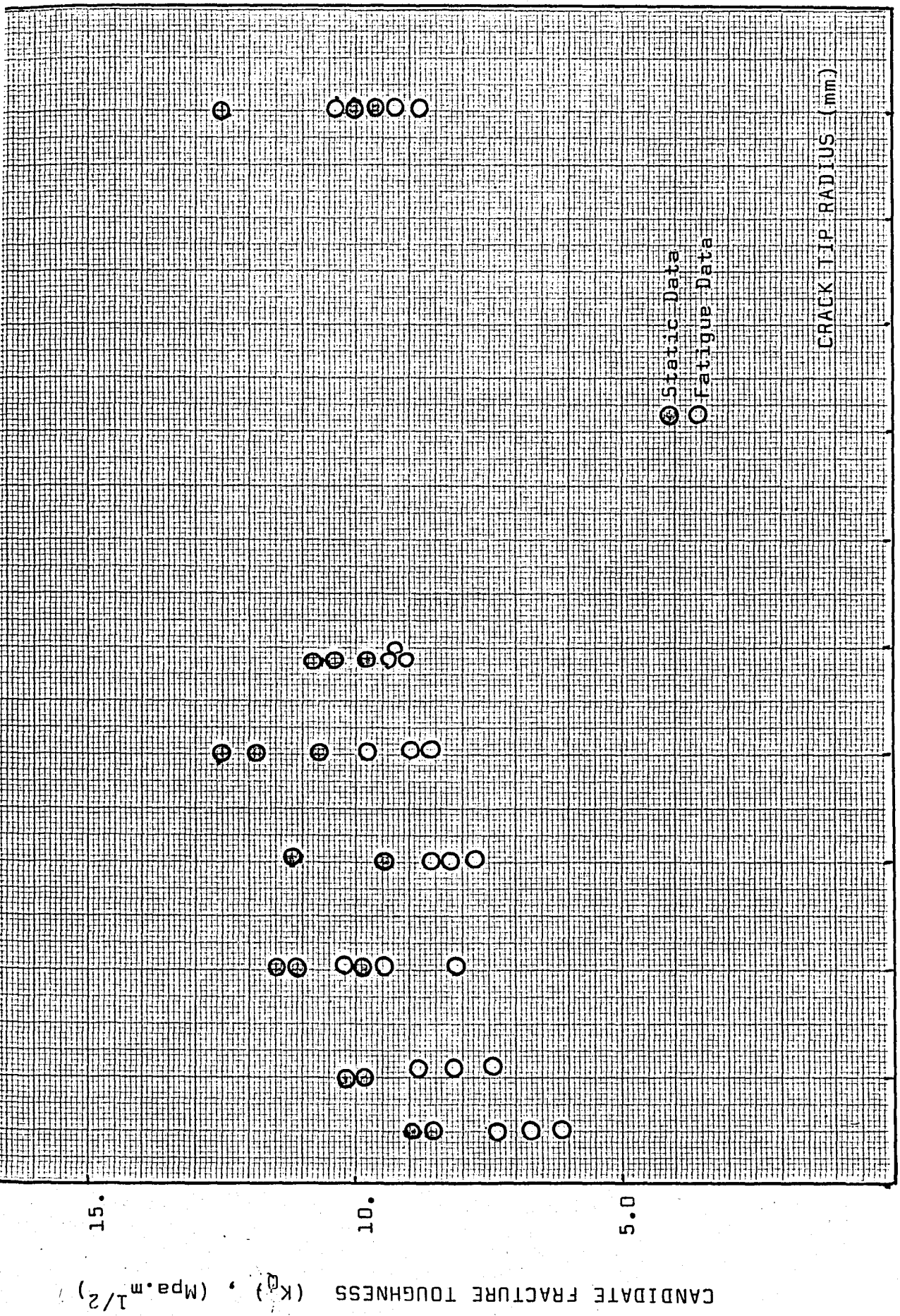

Figure 5.17 Cumulative Figure According To K_{1c} Testing Procedure

5.6.4 Mechanical Properties of the Laminate And Pure Matrix.

Table 5.11 and 5.12 gives the properties of the Laminate and Matrix materials used, respectively.

TABLE 5.11 Mechanical Properties of Glass fiber (Randomly oriented) Reinforced Polyster Resin (Glass w/o 32.8)

LAMINATE PROPERTIES			
	Tensile Strength	Elastic Modulus	Strain (%)
	(MPa)	(GPa)	
1	89.7	∿7.000	1.28
2	90.0	∿7.000	1.28
3	89.0	∿6.900	1.27

TABLE 5.12 Mechanical Properties of Matrix Material

MATRIX PROPERTIES		
Tensile Strength	Elastic Modulus	Strain (%)
(MPa)	(GPa)	
65-75	3.20	2.0-4.0

Polyster Neoxil 188N8 ortoftalik thermoset.

5.7 DISCUSSION OF RESULTS AND RECOMMENDATIONS

5.7.1 Static Tensile Testing Results

As mentioned before, the loads which are used to calculate σ_Q are chosen by three different methods. Figure 5.10 shows the result obtained according to the K_{IC} testing procedure. As seen, scattering is available but is less than that in the results obtained from the debonding approach and the unstable crack propagation approach.(Figure 5.11 and 5.12) Scattering occurs in all cases due to the nonhomogeneity of the material. Beyond the sharp notch, the material does not show any significant variation in stress intensity factor with increasing notch root radius if compared with metals and polymers. A smooth line can approximately be drawn through the points. It is, however difficult to say anything for $\rho < 0.25$ mm. A drop in toughness with sharper ρ, as seen in metals, is not excluded through this study. This notch root radius effect is more severe for "unidirectionally" reinforced carbon epoxy composites. (see figure 4.2)

Due to the composite character of the material, "sharp" notches may unavoidably lead to local effects. That is, many specimens should have been tested to get an "healthy" average value. The "sharp" notch ending right at a fiber or matrix or matrix/fiber interface may give quite different result. Thus, looking back now at the results, it is felt that more data are needed as one moves towards smaller ρ.

Debonding point approach is more conservative than the

others in general, but it yields scattered data Again, unstable crack propagation approach yields scattered data too and not convenient for calculating fracture toughness value, but it is easy to determine the load which is used in the calculation of the stress intensity factor, thus it can be useful for some engineering applications with a generous safety factor.

5.7.2 Fatigue Tensile Testing Results.

Figure 5.13, 5.14 and 5.15 show the effect of notch root radius on the fracture toughness of random glass fiber reinforced polyster resin after 10^5 cycles of fatigueing.

Scattering in data is observed again, but K_{IC} testing gives less scattering than the others. As in the case of the monotonic test results, the presence of a sharp notch loweres the fatigue strength data more than the other notch rood radii. Generally, beyond the sharp notch, it can be said that notch root radii in the range of 0.25 - 2.5 do not strongly affect the fracture toughness.

During fatigue, the damage zone developed at the notch tip does not create a sharp fatigue crack but it reduces fracture toughness of the material due to debonding. Examination of the fracture surfaces of the fatigued specimens shows some important points. In areas close to the notch tip, initiation of damage zone is closely related to the arrangement of local fiber strand.

As seen from figure 5.17, a significant decrease in fracture toughness value (Approximately 15-20% drop in K_Q after 10^5 cycles fatigueing) is observed in the fatigue case with respect

to the static case. This tendency is observed for all the three different ways of determining K_Q. Percent drop in K_Q is nearly the same for all approaches.

5.7.3 Static Tensile Testing Results of Pure Matrix

Sharply notched (ρ=0.125mm) and bluntly notched (ρ=1 mm) specimens failed in severely brittle manner in static tensile tests.

There is no plastic zone formation observed at the notch tip until fracture. The only difference between fracture of sharply and bluntly notched specimens is the fracture surface smoothness. The surfaces of the sharply notched specimens are very shiny and fracture surfaces of other specimens are relatively rough and opaque.

In addition, from figure 5.16 the dependence of fracture toughness on crack tip radius is obviously seen. Brittle matrix is known as notch root radius dependent. This was demonstrated by this study.

5.7.4 Recommended future work

For an investigation of the effect of cyclic loading on K_Q in detail, it is recommended to perform the tests of K_Q vs ρ at several N (number of cycles) typically $10^4, 10^5, 10^6$. We do not know whether there is a continuous drop in K_Q due to debonding. These tests can be repeated at several N for a different amplitude. It will be useful to discover the effects of amplitude and number of cycles to damage developed at the crack tip.

In addition to these, it is also recommended to investigate the effect of sharper notch radii (say, $\rho < 0.25$ mm) on K_Q.

VII. CONCLUSIONS

The following conclusions have been reached or verified as a direct result of investigations performed during this study.

1. For this class of random short fiber composites, the value of candidate fracture toughness (K_Q) is approximately independent of notch root radius between 0.25 to 2.5 mm.
2. Application of cyclic loading to the random glass fiber reinforced composites causes the candidate fracture toughness value to reduce considerably due to the formation of fatigue damage zone at notch tip.
3. Pure matrix (polyster resin) is notch tip radius dependent and shows very brittle fracture behavior
4. The results presented in this study suggest that K_{IC} testing concept can be a useful approach to study the fracture behavior of random fiber composites
5. Debonding point approach to find the K_Q gives more conservative values than do the other different methods used here.
6. Crack detection Compliance curve is recommended to measure the crack growth since surface observations do not yield a healthy average through the thickness.

APPENDIX - A

STRESS INTENSITY-FACTOR EQUATION

The stress-intensity-factor equation for a single edge notched (SE(T) specimen of finite width is given like that:

$$K_I = \sigma \sqrt{\pi a}\ f\left(\frac{a}{b}\right)$$

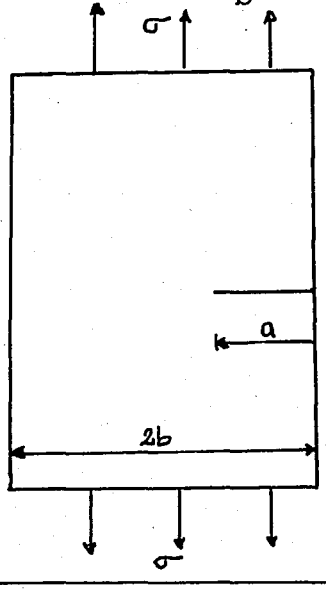

a/b	f(a/b)
0.1	1.15
0.2	1.20
0.3	1.29
0.4	1.37
0.5	1.51
0.6	1.68
0.7	1.89
0.8	2.14
0.9	2.46
1.0	2.86

Correction factors for a Single-Edge-Notched Plate (Barsom)

APPENDIX - B

The least Square Method and Computer Program

If points are convenient for a parabolic curve we can use the equation of

$$y = a_o + a_1 x + a_2 x^2$$

The least square equation

$$S = \sum_{i=1}^{N} (\bar{Y}_i - y_i)^2$$

or

$$S = \sum_{i=1}^{N} (a_o + a_1 x_i + a_2 x_i^2 - Y_i)^2$$

$$\text{if;} \quad \frac{\partial S}{\partial a_1} = \sum_{i=1}^{N} (a_o + a_1 x_i + a_2 x_i^2 - Y_i) = 0$$

$$\frac{\partial S}{\partial a_1} = \sum_{i=1}^{N} (a_o + a_1 x_i + a_2 x_i^2 - Y_i \cdot + x_i) = 0$$

$$\frac{\partial S}{\partial a_2} = \sum_{i=1}^{N} (a_o + a_1 x_i + a_2 x_i^2 - Y_i + X_i^2) = 0$$

in the reordering

$$Na_o + (\Sigma x_i)\, a_1 + (\Sigma x_i^2)\, a_2 = \Sigma Y_i$$

$$(\Sigma x_i)\, a_o + (\Sigma x_i^2) a_1 + (\Sigma x_i^3) a_2 = \Sigma x_i Y_i$$

$$(\Sigma x_i^2) a_o + (\Sigma x_i^3) a_1 + (\Sigma x_i^4) a_2 = \Sigma x_i^2 Y_i$$

in the matrix form;

$$\underset{M}{\begin{bmatrix} N & (\Sigma x_i) & (\Sigma x_i^2) \\ (\Sigma x_i) & (\Sigma x_i^2) & (\Sigma x_i^3) \\ (\Sigma z_i^2) & (\Sigma x_i^3) & (\Sigma x_i^4) \end{bmatrix}} \quad \underset{A}{\begin{bmatrix} a_o \\ a_1 \\ a_2 \end{bmatrix}} \quad \underset{N}{\begin{bmatrix} (\Sigma Y_i) \\ (\Sigma x_i Y_i) \\ (\Sigma x_i^2 Y_i) \end{bmatrix}}$$

The solution of the above matrix form gives the coefficients of the parabola.

```
list.f=comp
      PROGRAM COMPZ(INPUT,OUTPUT,TAPE5=INPUT,TAPE6=OUTPUT)
C
C  ***************************************************
C  *    MAIN PROGRAM                                 *
C  *                                                 *
C  *                                                 *
C  *    THIS PROGRAM MAKES A PARABOLIC FIT TO        *
C  *                                                 *
C  *    THE INPUT DATA USING LEAST-SQUARES METHOD    *
C  *                                                 *
C  *                                                 *
C  *                                                 *
C  *                                                 *
C  ***************************************************
      PARAMETER (N=27)
      REAL LP,LQ
      DIMENSION S(3,3),P(3,1),LP(3),LQ(3,2),R(3)
      DIMENSION X(N),Y(N),X1(50),Y1(50),X2(5,500),Y2(5,500),IN(5)
      DO 5  KK=1,1
      READ(5,*) (X(LI),LI=1,N)
      READ(5,*) (Y(LI),LI=1,N)
      DATA L,M,IFLAG/3,1,1/
      S(1,1)=N
      S(1,2)=0
      S(1,3)=0
      S(2,3)=0
      S(3,3)=0
      DO 10 I=1,N
      S(1,2)=S(1,2)+X(I)
      S(1,3)=S(1,3)+X(I)**2
      S(2,3)=S(2,3)+X(I)**3
      S(3,3)=S(3,3)+X(I)**4
      S(2,1)=S(1,2)
      S(3,1)=S(1,3)
      S(2,2)=S(1,3)
      S(3,2)=S(2,3)
 10   CONTINUE
      P(1,1)=0
      P(2,1)=0
      P(3,1)=0
      DO 7 I=1,N
      P(1,1)=P(1,1)+Y(I)
      P(2,1)=P(2,1)+X(I)*Y(I)
      P(3,1)=P(3,1)+X(I)**2*Y(I)
  7   CONTINUE
      WRITE(6,12) ((S(I,J),J=1,3),I=1,3)
 12   FORMAT(1H1,10X,'MATRIX M ',//,3(E10.3,1X))
      WRITE(6,13) (P(I,1),I=1,3)
 13   FORMAT(//,10X,'VECTOR N',//,3(F8.2,1X))
      CALL GAUSS(S,P,L,M,IFLAG,LP,LQ,R)
      WRITE(6,15) (P(I,1),I=1,3)
 15   FORMAT(//,10X,'COEFFICIENTS',//3(F8.2,1X))
      X1(1)=10.
      DO 20 I=1,20
      Y1(I)=P(1,1)+P(2,1)*X1(I)+P(3,1)*X1(I)**2
 20   X1(I+1)=X1(I)+1
      DO 25 I=1,50
      X2(KK,I)=X1(I)
 25   Y2(KK,I)=Y1(I)
      WRITE(6,123) (X2(1,I),I=1,50)
      WRITE(6,124) (Y2(1,I),I=1,50)
123   FORMAT(//,3X,50(F8.2,//))
```

```
      IN(1)=20
      IN(2)=20
      IN(3)=20
    5 CONTINUE
      CALL GRAFIC (111,56,X2,Y2,IN,0,1)
      STOP
      END
C
C     ************************
C     * SUBROUTINE GAUSS     *
C     ************************
C
      SUBROUTINE GAUSS (S,P,L,M,IFLAG,LP,LQ,R)
      DIMENSION S(3,3),P(3,1),LP(3),LQ(3,2),R(3)
      DO 11 I=1,L
   11 LP(I)=0
      DO 150 K=1,L
      CON=0
      DO 50 I=1,L
      IF(LP(I).EQ.1) GO TO 50
      DO 40 J=1,L
      IF(LP(J)-1) 30,40,200
   30 IF(ABS(CON).GE.ABS(S(I,J))) GO TO 40
      IR=I
      IC=J
      CON=S(I,J)
   40 CONTINUE
   50 CONTINUE
      LP(IC)=LP(IC)+1
      IF(IR.EQ.IC) GO TO 90
      DO 60 I=1,L
      CON=S(IR,I)
      S(IR,I)=S(IC,I)
   60 S(IC,I)=CON
      IF(IFLAG.EQ.0) GO TO 90
      DO 70 I=1,M
      CON=P(IR,I)
      P(IR,I)=P(IC,I)
   70 P(IC,I)=CON
   90 LQ(K,1)=IR
      LQ(K,2)=IC
      R(K)=S(IC,IC)
      S(IC,IC)=1
      DO 100 I=1,L
  100 S(IC,I)=S(IC,I)/R(K)
      IF(IFLAG.EQ.0) GO TO 120
      DO 110 I=1,M
  110 P(IC,I)=P(IC,I)/R(K)
  120 DO 150 I=1,L
      IF(I.EQ.IC) GO TO 150
      CON=S(I,IC)
      S(I,IC)=0
      DO 130 J=1,L
  130 S(I,J)=S(I,J)-S(IC,J)*CON
      IF(IFLAG.EQ.0) GO TO 150
      DO 140 II=1,M
  140 P(I,II)=P(I,II)-P(IC,II)*CON
  150 CONTINUE
      DO 170 I=1,L
      J=L-I+1
      IF(LQ(J,1).EQ.LQ(J,2)) GO TO 170
      IR=LQ(J,1)
      IC=LQ(J,2)
      DO 160 K=1,L
      CON=S(K,IR)
```

```
      S(K,IR)=S(K,IC)
      S(K,IC)=CON
  160 CONTINUE
  170 CONTINUE
  200 RETURN
      END
C***SUBROUTINE GRAFIC*************************************************
C
C     IX     : DIMENSION OF X
C     IY     : DIMENSION OF Y
C     X      : INDEPENDANT VARIABLE
C     Y      : DEPENDANT VARIABLE
C     IN     : NUMBER OF POINT
C     NL     : LOGARITMIC INDICATOR(NL=0 X AND Y NORMAL,NL=1 X AND Y LOGARIT
C              NL=2  ONLY X LOGARITMIC,NL=3 ONLY Y LOGARITMIC)
C     IDIM   : NUMBER OF GRAFIC
C
C***SUBROUTINE GRAFIC***X*Y*X*Y*N*NL*IDIM*****************************
      DIMENSION X(5,500),Y(5,500),U(111),V(56),D(12),E(12),IN(5)
      CHARACTER *1 A(56,111),F(111)*1
      REAL MIN,MIN1,MAX,MAX1,INCX,INCY
      DO 5 I=1,56
      DO 5 J=1,111
      A(I,J)=' '
    5 CONTINUE
      IF(IX.GT.111.OR.IX.LT.2) IX=111
      IF(IY.GT.56.OR.IY.LT.2) IY=56
      IF(NL.EQ.1.OR.NL.EQ.2) THEN
      DO 10 M=1,IDIM
      DO 10 I=1,IN(M)
      IF(X(M,I).NE.0) THEN
      X(M,I)=ALOG10(X(M,I))
      ENDIF
   10 CONTINUE
      END IF
      IF(NL.EQ.1.OR.NL.EQ.3) THEN
      DO 15 M=1,IDIM
      DO 15 I=1,IN(M)
      IF(Y(M,I).NE.0) THEN
      Y(M,I)=ALOG10(Y(M,I))
      ENDIF
   15 CONTINUE
      END IF
      DO 20 I=1,IX
      F(I)='-'
   20 CONTINUE
      DO 25 I=1,IX,10
      F(I)='+'
   25 CONTINUE
      MIN=X(1,1)
      MAX=X(1,1)
      MIN1=Y(1,1)
      MAX1=Y(1,1)
      DO 35 M=1,IDIM
      DO 30 I=1,IN(M)
      IF(X(M,I).GT.MAX) MAX=X(M,I)
      IF(X(M,I).LT.MIN) MIN=X(M,I)
      IF(Y(M,I).GT.MAX1) MAX1=Y(M,I)
      IF(Y(M,I).LT.MIN1) MIN1=Y(M,I)
   30 CONTINUE
   35 CONTINUE
      INCX=(MAX-MIN)/(IX-1)
      INCY=(MAX1-MIN1)/(IY-1)
      U(1)=MIN
      V(1)=MIN1
```

```
      U(I+1)=U(I)+INCX
   40 CONTINUE
      DO 45 I=1,IY-1
      V(I+1)=V(I)+INCY
   45 CONTINUE
      DO 65 M=1,IDIM
      DO 60 I=1,IN(M)
      M1=1
      DIFF=ABS(X(M,I)-U(1))
      DO 50 J=1,IX-1
      IF(ABS(X(M,I)-U(J+1)).LT.DIFF) THEN
      DIFF=ABS(X(M,I)=U(J+1))
      M1=J+1
      END IF
   50 CONTINUE
      L=1
      DIFF1=ABS(Y(M,I)-V(1))
      DO 55 J=1,IY-1
      IF(ABS(Y(M,I)-V(J+1)).LT.DIFF1) THEN
      DIFF1=ABS(Y(M,I)-V(J+1))
      L=J+1
      END IF
   55 CONTINUE
      IF(M.EQ.1) A(L,M1)='+'
      IF(M.EQ.2) A(L,M1)='.'
      IF(M.EQ.3) A(L,M1)='*'
      IF(M.EQ.4) A(L,M1)='G'
      IF(M.EQ.5) A(L,M1)='&'
   60 CONTINUE
   65 CONTINUE
      L2=0
      L3=0
      DO 70 I=1,IY,5
      L2=L2+1
      IF(NL.EQ.1.OR.NL.EQ.3) D(L2)=10**V(I)
      IF(NL.NE.1.AND.NL.NE.3) D(L2)=V(I)
   70 CONTINUE
      DO 75 I=1,IX,10
      L3=L3+1
      IF(NL.EQ.1.OR.NL.EQ.2) E(L3)=10**U(I)
      IF(NL.NE.1.AND.NL.NE.2) E(L3)=U(I)
   75 CONTINUE
      IF(NL.EQ.1.OR.NL.EQ.2) THEN
      DO 80 M=1,IDIM
      DO 80 I=1,IN(M)
      X(M,I)=10**X(M,I)
   80 CONTINUE
      END IF
      IF(NL.EQ.1.OR.NL.EQ.3) THEN
      DO 85 M=1,IDIM
      DO 85 I=1,IN(M)
      Y(M,I)=10**Y(M,I)
   85 CONTINUE
      END IF
      K7=((IY-1)/5)*5+1
      IP=(IX-1)/10+1
      PRINT 95
      DO 90 I=IY,1,-1
      IF(I.EQ.K7) THEN
      K7=K7-5
      L=I/5+1
      PRINT 100, D(L),(A(I,J),J=1,IX)
      GO TO 90
      END IF
      PRINT 105, (A(I,J),J=1,IX)
```

```
   90  CONTINUE
       PRINT 110, (F(I),I=1,IX)
       PRINT 115, (E(I),I=1,IP)
       RETURN
   95  FORMAT(1H1,/)
  100  FORMAT(3X,1PE10.2,1X,'+',111A1)
  105  FORMAT(14X,'I',111A1)
  110  FORMAT(15X,111A1,/)
  115  FORMAT(11X,11(1PE9.2,1X),1PE9.2,/)
       END
```


8.91E+00
7.89E+00
6.88E+00
5.87E+00
4.86E+00
3.85E+00
2.84E+00
1.83E+00
1.00E+01
1.28E+01
1.55E+01
1.83E+01
2.10E+01
2.38E+01
2.65E+01

APPENDIX - C

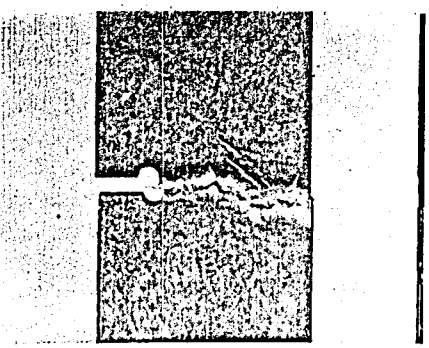

a_o=15 mm, ρ=2.5 mm

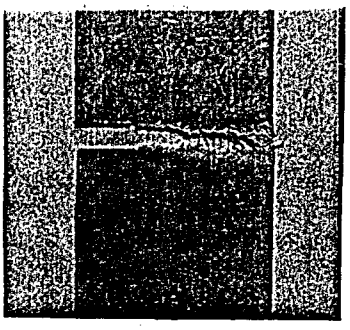

a_o=15 mm, ρ=1.15 mm

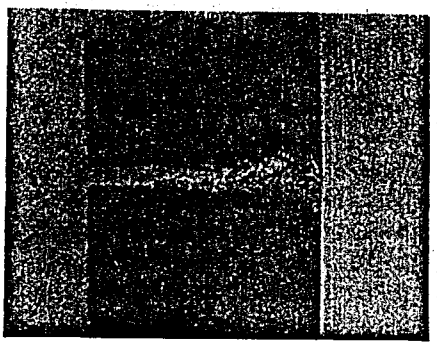

a_o=15 mm, ρ=1.0 mm

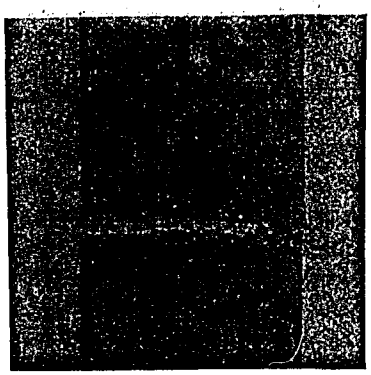

a_o=15 mm, ρ=0.75 mm

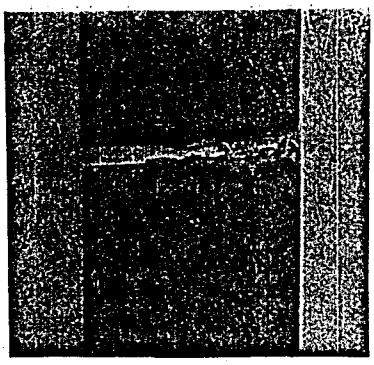

a_o=15 mm, ρ=0.50mm

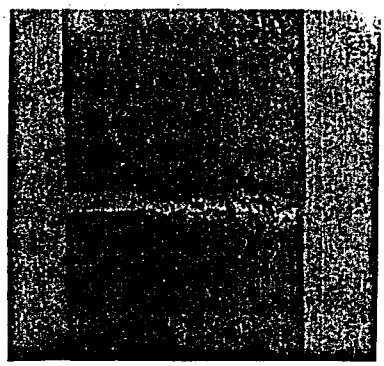

a_o=15 mm, ρ=0.25

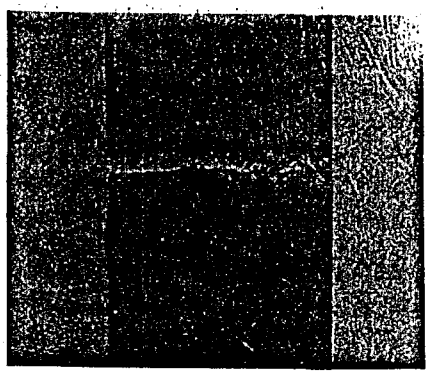

a_o=15 mm, ρ=sharp(0.125)

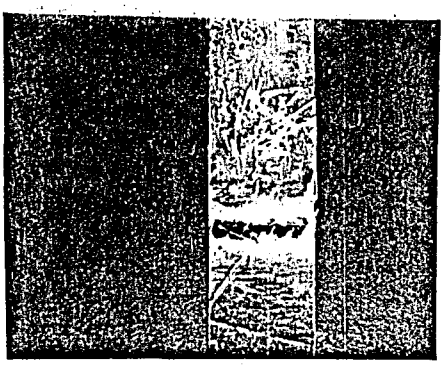

Tension Specimen

REFERENCES

1. E.M.Wu; "Fracture Mechanics of An isotropic Plates", composite material workshop, technomic Publishing C_o,pp.100-121(1983)

2. P.W.R. Beamont and D.C. Phillips; "The fracture energy of a glass fiber composite"; A report of Materials Dep., school of Eng. and Applied Science, University of California, (1967)

3. S.Gaggar,LJ. Broutman: "Fracture toughness of random glass fiber epoxy composites", Flow Growth and Fracture, ASTM STP 631, pp 311-329 (1977)

4. S.Gaggar, LJ.Broutman; "Crack Growth Resistance of Random Fiber Composites", Report of Dep. of Metallurgical and Materials Eng., Illinois Institute of Technology, Chicago, (1975)

5. M.J.Oven, P.T.Bishop; "Critical Stress Intensity Factors Applied to Glass Reinforced Polyster Resin", J.Composite Materials, vol 7, pp. 146-12,(1973)

6. S.S.Wang, ESM Chim, T.P.Yu and D.P. Goetz; "Fracture of Random Short Fiber SMC composite", J.of composite Mater. vol.17, pp.299-308 July (1983)

7. M.J.Owen,P.T Bishop; "Crack Growth Relationships For Glass Reinforced Plastics and their application to design," J.Phys D. Applied Phys, vol 17, pp 146-151 (1974)

8. M.H.Sadd, S.G Mc Daniel, K.E.Tucker, "The effect of fatigue on the fracture strength of PMMA", Int.J. of Fracture,14, pp.430-437 (1978)

9. J.M.Mandell; "Fatigue behavior of fiber-resin composites", Polymer composites, vol.2, no 1, January (1981).

10. M. Takano,L.ENielsen; "The notch sensitivity of polymeric Materials", J. Applied Polymer Science, vol-20,pp.2193-2207, (1976)

11. M.J.Owen, R.G.Rose; "Failure mechanisms in reinforced plastics with short randomly distributed fibers", Plastics and Polymers, Dec. pp 325-329 (1972)

12. D.Denton;" Mechanical Properties Characterization of an SMC-50 Composite", 34 th Annual Technical Conference, SPI, 11-F, (1979)

13. R.Hertzberg, J.Manson,"Fatigue of Eng. Plastics", p.185, Academic Press, USA,(1980)

14. H.Liebowitz; "Fracture, an Advanced Treatise", vol 7, p 676, Academic Press, New York, (1972)

15. R.Hertzberg; "Deformation and Fracture Mechanics of Engineering Materials", Academic Press, pp.46-51, USA (1976).

16. T.Misaki and J.Kishi; "Effects of notches and Glass fiber reinforcement on fatigue behavior of PC', J. of Applied Pol. Science, vol 22, pp.2063-2067, (1978).

17. C.D. Ellis and B. Harris; "The effect of specimen and Testing variables on the fracture of some fiber reinforced epoxy resins", J.composite Mater., vol 7, pp 76-79, (1973)

18. S.Gaggar and L.J.Broutman; "The development of a damage zone at the tip of a crack in a glass fiber reinforced Polyster resin", Int. J. Fracture, vol 10, pp 606-608, (1974)

19. TN.Y. Owen, "Fatigue Damage in glass fiber reinforced plastics", Dep. of Mechanical Eng., The University of Nottingham, England, Report (1973)

20. B.Harris : "Fatigue Testing of Fiber Composites", school of Materials science, university of Bath, U.K. Report,(1980)

21. S.Z.Wang and E.S.M Chim. "Fatigue Damage and Degradation in Random Short-fiber SMC Composites", J.Composite Mater, Vol. 17, pp 356-362 May (1983)

22. S.S.Wang,E.S.M Chim, N.M.Zahlan; "Fatigue Crack Propagation in Random short fiber SMC composite", J.composite Materials, Vol 17, pp 146-149 March (1983)

23. G.C.Sih, P.A. Thorton, "Fracture of the Composite materials", J.composite Materials, Vol 6, pp 147-151, (1972)